Artificial Intelligence Review (2022) 55:6389–6459
https://doi.org/10.1007/s10462-022-10157-w

A new fusion of whale optimizer algorithm with Kapur's entropy for multi-threshold image segmentation: analysis and validations

Mohamed Abdel-Basset[1] · Reda Mohamed[1] · Mohamed Abouhawwash[2,3]

/ Published online: 21 March 2022

Abstract
The separation of an object from other objects or the background by selecting the optimal threshold values remains a challenge in the field of image segmentation. Threshold segmentation is one of the most popular image segmentation techniques. The traditional methods for finding the optimum threshold are computationally expensive, tedious, and may be inaccurate. Hence, this paper proposes an Improved Whale Optimization Algorithm (IWOA) based on Kapur's entropy for solving multi-threshold segmentation of the gray level image. Also, IWOA supports its performance using linearly convergence increasing and local minima avoidance technique (LCMA), and ranking-based updating method (RUM). LCMA technique accelerates the convergence speed of the solutions toward the optimal solution and tries to avoid the local minima problem that may fall within the optimization process. To do that, it updates randomly the positions of the worst solutions to be near to the best solution and at the same time randomly within the search space according to a certain probability to avoid stuck into local minima. Because of the randomization process used in LCMA for updating the solutions toward the best solutions, a huge number of the solutions around the best are skipped. Therefore, the RUM is used to replace the unbeneficial solution with a novel updating scheme to cover this problem. We compare IWOA with another seven algorithms using a set of well-known test images. We use several performance measures, such as fitness values, Peak Signal to Noise Ratio, Structured Similarity Index Metric, Standard Deviation, and CPU time.

Keywords Image segmentation · Whale optimization algorithm · Linearly convergence · Local Minima · Kapur's entropy

✉ Mohamed Abouhawwash
saleh1284@mans.edu.eg; abouhaww@msu.edu

Extended author information available on the last page of the article

1 Introduction

Image segmentation is the practice of splitting an image into several homogeneous and continuous regions that do not overlap so that any two of these regions are heterogeneous. It is a mandatory step in image processing (Kuruvilla et al. 2016) and computer vision (Hu et al. 2016) to facilitate the analysis and understanding of images. Recently, there are various types of images to be processed and analyzed, such as X-ray (Zhang et al. 2020), Nuclear Magnetic Resonance (NMR) (Griswold et al. 2019), computed tomography (Farook et al. 2020; Zhang et al. 2020), sonar (Song and Liu 2020), position emission tomography (Bal et al. 2020), thermal (Al-Musawi et al. 2020), light intensity (gray-scale), and color images. Several image segmentation approaches have been developed, including region detection (Aksac et al. 2017), edge detection (Prathusha and Jyothi 2018), Feature selection-based clustering (Narayanan et al. 2019), and threshold segmentation (Han et al. 2017).

Threshold segmentation is one of the most commonly used approaches categorized into bi-level threshold and multi-level threshold. In the bi-level threshold, we can group image objects into two classes: foreground (object) and background. When the image contains different objects with different intensity, the bi-level threshold couldn't segment it. Accordingly, we use a more complex threshold segmentation called a multi-level one. The multi-level threshold groups the image objects into more than two classes. Threshold segmentation is simple, accurate, fast, and needs small storage. Unfortunately, time complexity increases exponentially with the multi-level threshold. The used threshold techniques try to find the optimal threshold values based on two approaches: parametric and non-parametric approaches (Dirami et al. 2013). In the parametric approach, each class in the image has some parameters to be calculated using a probability density function. The non-parametric one obtains the threshold values by maximizing some of those functions (Kapur's entropy (Kapur et al. 1985), fuzzy entropy (Oliva et al. 2019), and Otsu method (Otsu 1979; Bhandari and Kumar 2019)) without using statistical parameters.

The traditional techniques used to find the optimal threshold values are time-consuming. Meta-heuristic algorithms have been used and integrated with threshold segmentation techniques to overcome the high time complexity for a multi-level threshold. Many authors pay attention to employ meta-heuristic algorithms for solving multi-threshold segmentation problems, including Genetic Algorithm (GA) (Elsayed et al. 2014), Particle Swarm Optimization (PSO) (Guo and Li 2007; Xiong et al. 2020; Di Martino and Sessa 2020), ant-colony optimization algorithm (Kaveh and Talatahari 2010), Whale Optimization Algorithm (WOA) (Abd El Aziz et al. 2017), symbiotic organisms search optimization (Chakraborty et al. 2019), and firefly optimization (Erdmann et al. 2015).

Unfortunately, the algorithms in the literature for the ISP suffer at least from one of the following problems:

- Falling into local minima,
- Low convergence speed,
- Not feasible for tackling images having higher threshold levels.

Therefore, in this paper, a new optimization approach based on the improved whale optimization algorithm is proposed to overcome the previous drawbacks for the ISP.

Recently, a new optimization algorithm (Mirjalili and Lewis 2016), namely whale optimization algorithm (WOA), has been proposed for tackling continuous optimization problems. Although the significant performance of the WOA in reaching good outcomes for several real optimization problems (Abdel-Basset et al. 2020; Jafari-Asl et al. 2021; El-Fergany et al. 2019), it still suffers from the local minima and the low convergence speed. Therefore, in this paper, WOA is improved using two strategies to promote its exploration and exploitation capabilities. The first strategy is the linearly convergence increasing and local minima avoidance technique (LCMA) that moves the positions of the worst solutions to be near to the best solution and at the same time randomly within the search space of the problem to avoid falling into local minima. The second strategy is the ranking-based updating method (RUM) to replace the unbeneficial solutions with other better solutions, helping in improving its performance. After then, these strategies are effectively integrated with the standard WOA to maximize Kapur's entropy for tackling the ISP. Empirically, the improved WOA (IWOA) is validated 13 test images taken from Berkeley Segmentation Dataset (BSD) with threshold levels between 2 and 100 to check the efficacy of IWOA in selecting the optimal thresholds. To see the superiority of the proposed algorithm, it is compared with a number of well-known optimization algorithms under various performance metrics: SSIM, PSNR, STD, fitness value, and CPU time. The empirical outcomes prove the efficacy of IWOA on these images in comparison to the compared optimization algorithms for SSIM, PSNR, STD, and the values of the objective. Unfortunately, the proposed algorithm couldn't overcome some compared algorithms for the CPU time as our main limitations, but its superiority for the other metrics, such as SSIM, PSNR, and STD makes a better alternative for the existing method proposed for ISP. Finally, we summarize the main contributions of this paper as follows:

- We propose an Improved Whale Optimization Algorithm (IWOA) based on Kapur's entropy for solving the multi-threshold image segmentation.
- We improve the performance of IWOA using the LCMA, and RUM.
- Several experiments and the Wilcoxon rank-sum test are conducted to prove the efficacy of IWOA in comparison with other well-known algorithms based on some performance metrics, including Peak Signal to Noise Ratio (PSNR), Structured Similarity Index Metric (SSIM), and fitness value metrics using a set of benchmark test images.

We organize the remaining of the paper as follows. Section 2 presents the previous works done for tackling the multi-threshold image segmentation problem. In Sect. 3, we introduce the multi-threshold image segmentation problem using Kapur's entropy. Moreover, Sect. 4 describes the whale optimization algorithm. Section 5 explains and illustrates the proposed algorithm. Section 6 shows the experiments outcome and their discussions. Finally, Sect. 7 draws the conclusions and the future works about the proposed algorithm.

2 Related work

Image segmentation groups the pixels of an image according to some specific criteria, including textures, shape, color, and intensity. Many applications exploit image segmentation in understanding and analyzing the acquired images, such as medical diagnosis (Mittal et al. 2020; Zhang et al. 2020; Sinha et al. 2020; Ren et al. 2019), object recognition (Wang et al. 2019), geographical imaging (Chen 2020), satellite image processing (Karydas 2020), remote sensing (Su and Zhang 2017), historical documents (Alberti et al. 2017), and historical newspapers (Naoum et al. 2019; Barman et al. 2020). Although threshold segmentation is easy to implement and has a low computational burden, it is still a challenge for the researchers to determine the optimal n- level threshold. The traditional methods to search for optimal thresholds values such as an exhaustive search can be tedious and computationally expensive. Many authors handled the problem of n- level threshold as an optimization problem solved using meta-heuristic algorithms, which could overcome several optimization problems (Abdel-Basset et al. 2020a, b, [44], Abdel-Basset et al. 2020; Lang and Jia 2019). We will review several attempts done for the optimal threshold selection.

Singla and Patra (2017) selected the initial thresholds by obtaining the mid-points of any two consecutive peaks of the energy curve of an image. Then, the cluster validity measure tries to find the potential thresholds and the bounds that may contain the optimal ones. Finally, the GA algorithm seeks to discover the optimal thresholds from its defined bounds. Also, Manikandan et al. (2014) proposed GA with a simulated binary crossover to maximize the Kapur's entropy for medical image segmentation. Another meta-heuristic algorithm PSO introduced for image segmentation. Maitra and Chatterjee (2008) integrated PSO with cooperative and comprehensive learning to face the dimensionality curse and to reduce the premature convergence of the swarm, respectively. Consequently, a modified PSO (Liu et al. 2015) employed the adaptive inertia and the adaptive population to improve its performance for maximizing the Otsu's function to find the optimal thresholds, which will separate homogenous regions within an image. The MPSO has been validated on 12 test images and compared with the standard PSO and GA. Ghamisi et al. (2013) introduced fractional-order Darwinian PSO to solve the problem of the n-level threshold based on Otsu to maximize the variance between the classes.

Another metaheuristic is the Bacterial Foraging Algorithm (BFA). Sanyal et al. (2011) applied an adaptive BFA for gray-scale image segmentation depending on fuzzy entropy, which adaptively switches the bacterium between exploitation and exploration stages. Also, the authors in Sathya and Kayalvizhi (2011) accelerated the convergence of a modified BFA by moving the best bacteria to the subsequent iterations. The results proved that the modified BFA based on Otsu's function has a high convergence speed in comparison with Kapur's one. After that, a cooperative BFA (Liu et al. 2015) combined a self-adaptive foraging strategy, which controls the swim amplitude and cell-to-cell communication. The cooperative BFA had higher quality segmentation and less CPU time. Furthermore, BFA (Tang et al. 2017) is incorporated with PSO to support the global search capability in addition to the weak bacterium, which selects a random strong one to reach a location near it. Pan et al. (2017) developed BFA depending on edge-detection for cell image segmentation as the traditional edge-detection techniques are costly expensive and may produce disconnected edges. Lately, BFA (Wang et al. 2019) is integrated with PSO to avoid randomly selecting the direction of the bacterial chemotactic step.

Mostafa et al. (2017) proposed a liver image segmentation using WOA that multiplies the clustered image by the binary one. This clustered image divides the liver image into a predetermined number of clusters. Also, the algorithm used the statistical image to indicate the liver position and converted it into a binary one. The problem of multi-level threshold segmentation (Abd El Aziz et al. 2018) is handled as a multi-objective problem that maximized both the Kapur's entropy and Otsu's function. Abd El Aziz et al. (2017) examines the performance of the WOA and Moth-Flame Optimization (MFO) algorithm. WOA traps into local optima while MFO succeeds in balancing the switch between the exploration and the exploitation phases (Sikariwal and Chanak 2018). Ultimately, some of the most recent multilevel thresholds image segmentation method are briefly discussed in Table 1.

Table 1 Some recent methods proposed for ISP

Algorithms	Contributions and disadvantages
Hybrid slime mould optimizer with whale optimization algorithm (HSMA_WOA) (Abdel-Basset et al. 2020)	Contributions – This paper proposed a new image segmentation algorithm based on integrating the slime mould algorithm (SMA) with the whale optimization algorithm for segmenting the Covid-19 X-ray images – This approach employed both SMA and WOA together to unify their advantages for overcoming the disadvantages of each one separately – Afterward, HSMA_WOA has validated 12 chest X-ray images and its outcomes were compared with those of a number of well-known optimization algorithms to see their efficacy – Finally, the experimental findings show the superiority of the HSMA_WOA over the others Disadvantages – Its performance for general test images has not been observed
An equilibrium optimizer (EO) (Abdel-Basset et al. 2021)	Contributions – In this paper, the equilibrium optimizer was adapted for the multilevel thresholding image segmentation problem by maximizing Kapur's entropy to find the optimal threshold values for various threshold levels – It has been validated using a number of images and compared to some well-known optimization algorithms to appear its efficacy Disadvantages – Still suffers from falling inside local minima which prevents it from reaching the optimal threshold values
Improved marine predators algorithm (IMPA) (Abdel-Basset et al. 2020)	Contributions – Recently, a novel multilevel thresholding image segmentation approach has been proposed for segmenting the Covid-19 X-ray images – This approach was based on the marine predators algorithm improved by a ranking-based diversity reduction strategy to increase the exploitation capability of the standard marine predators algorithm – The experimental outcomes proved the superiority of this improved one in terms of PSNR, SSIM, standard deviation, fitness values, and UQI Disadvantages – A little expensive in terms of the computational cost compared to the standard MPA and some of the rival algorithms

Table 1 (continued)

Algorithms	Contributions and disadvantages
Antlion optimization (ALO) and multiverse optimization (MVO) algorithms (Chouksey et al. 2020)	Contributions – In this paper, both ALO and MVO have been proposed for overcoming the multilevel thresholding image segmentation problem by maximizing both Kapur's entropy and the Otsu method – Those two algorithms were compared with other evolutionary methods in terms of PSNR, SSIM, feature similarity index (FSIM), standard deviation, stability analysis, and fitness values. The experimental results showed that MVO is faster and better than the compared methods Disadvantages – Its performance for threshold levels higher than 5 is not known and hence not preferred for the images that have threshold levels higher than that
An improved Bloch quantum artificial bee colony algorithm (ABC) (Huo et al. 2020)	Contributions – The ABC has been improved by the quantum Bloch spherical coordinates of the qubit for reaching better outcomes within a small number of iterations when solving the multilevel thresholding image segmentation problem – The experimental outcomes show the superiority of the proposed algorithm Disadvantages – Low convergence speed – Falling into local minima
Coyote optimization algorithm (COA)(Moses 2020)	Contributions – In this paper, the COA was adapted to tackle the ISP – The experimental outcomes showed the superiority of the COA in terms of convergence speed, objective values, and image quality Disadvantages – Moves slowly to the near-optimal solution and this will make it consume several function evaluations
Crow search algorithm (CSA) (Moses et al. 2019)	Contributions – Those authors proposed the CSA with the Otsu method as an objective function for selecting the optimal threshold values – The CSA proved its superiority over the improved particle swarm optimization (PSO), firefly algorithm (FFA), and also the fuzzy version of FA in terms of the quality of the segmented image, and the objective values Disadvantages – Low convergence speed – Not observed for threshold levels greater than 5

Table 1 (continued)

Algorithms	Contributions and disadvantages
Modified water wave optimization (MWWO) algorithm (Yan et al. 2020)	Contributions – In this paper, the water wave optimization algorithm was modified by the opposition-based learning strategy and ranking-based mutation strategy to find the optimal values for the underwater image segmentation problem – The opposition-based learning was used to increase the diversity of the individuals to avoid being stuck into local minima and reach better outcomes. While the ranking-based mutation operator was used to improve the selection probability – The experimental results showed the superiority of MWWO in terms of the segmented images and the objective values over the other compared algorithms Disadvantages – Not compared with the recently-published algorithms where the latest compared algorithm was published in 2017
Modified Red Deer Algorithm (MRDA) (De et al. 2020)	Contributions – The red deer algorithm modified by a few adaptive approaches to improve its efficacy has been proposed in this research for tackling the image segmentation problem – This algorithm was compared with the standard one and genetic algorithm over a set of real-life test images and could prove its efficacy in terms of fitness value, convergence speed, and standard deviation Disadvantages – Not investigated using several test images to check its stability, in addition to using a huge number of iteration up to 1000 which notifies its low convergence speed in the right direction of the near-optimal solution
Modified hybrid bat algorithm (Yue and Zhang 2020)	Contributions – Recently, the bat algorithm has been modified by a genetic crossover operator and a smart inertia weight (SGA-BA) to enhance its performance for maximizing the Otsu method to estimate the optimal thresholds of a set of images Disadvantages – Consuming computational cost higher than the other compared algorithm

Table 1 (continued)

Algorithms	Contributions and disadvantages
Improved flower pollination optimizer (IFPA) (Li and Tan 2019)	Contributions – In this paper, the authors improved the flower pollination algorithm for optimizing the Tsallis entropy as an objective function to find the optimal thresholds that separate similar regions within an image – The experimental results show the superiority of this improved one compared to those three algorithms
Grey Wolf Optimizer (GWO)(Khairuzzaman and Chaudhury 2017)	Contributions – The GWO has been proposed for finding the optimal thresholds to separate similar regions within an image. This algorithm used Kapur's entropy and Otsu method as objective functions to find those optimal thresholds – The experimental results show that GWO could be superior in terms of the quality of segmented images and stability and speed Disadvantages – Using the intensity of the image to perform the segmentation process – Not adequate for the images having intensity inhomogeneity problem

Many other meta-heuristic algorithms are developed for image segmentation, such as cuckoo search (Bhandari et al. 2014), bat algorithm (Yue and Zhang 2020), flower pollination algorithm (Wang et al. 2015), crow search algorithm (Oliva et al. 2017; Upadhyay and Chhabra 2019), Harris hawk optimization algorithm (Bao et al. 2019), grey wolf optimizer (Yao et al. 2019), krill herd algorithm (He and Huang 2020), bee colony algorithm [59], multi-verse optimizer (Kandhway and Bhandari 2019), and locust search algorithm (Cuevas et al. 2020). Unfortunately, the traditional methods for threshold image segmentation are costly in terms of computations and time-consuming. Therefore, many of the researchers find themselves forced to search for new ways to solve this problem in less time and not computationally expensive. One of these ways is to deal with threshold image segmentation as an optimization problem that can be solved using meta-heuristic algorithms. However, the success of meta-heuristic algorithms in obtaining an optimal solution in a reasonable time, the balance between the exploration and exploitation phases and falling into local optima are the biggest problem to face when dealing with theses algorithms. Also, the convergence speed of the algorithms toward the optimal solution may be slow.

As a result, this paper comes to address the aforementioned drawbacks and solve the problem of threshold image segmentation. WOA is one of the meta-heuristic algorithms that are applied to many problems (Mafarja and Mirjalili 2018; Liu et al. 2020; Abdel-Basset et al. 2018). This motivates us to propose an improved whale optimization algorithm that employs the LCMA technique for tackling threshold image segmentation. LCMA works on solving two problems that the WOA suffers from. WOA at the start has high exploration capability and reduces gradually with the iteration; this is considered the first problem due to reducing the convergence speed within the starting of the optimization process. After finishing the exploration capability, which after the first half of the iteration, the WOA will pay attention to the best-so-far solution to find a better solution around it if it is not local minima and this is considered the second problem. Accelerating the convergence speed of the algorithm toward the best-so-far and avoiding falling into local minima motivate us to propose LCMA to move the locations of K worst individuals near to the location of the best one and randomly within the search space according to a certain probability, in addition to using the ranking-based updating method (RUM) to replace the unbeneficial solutions with other solutions generated based on a novel scheme helping the algorithm in exploiting more solutions around the best-so-far solutions. K, at the start, carries a small value, and this value increases gradually with the iteration until getting to the maximum (all the individuals in the population) at the ending of the optimization process. Kapur's entropy illustrated in the following section is used to evaluate the quality of the solutions.

3 Mathematical model of Kapur's entropy

Kapur's entropy (Kapur et al. 1985) is a method that works on finding the optimal threshold values that will separate the similar regions within an image by maximizing the entropy of the histogram. Let's start with a bi-level threshold. In bi-level threshold, this method tries to find the threshold value t that divides an image into background and foreground, namely, B and F that maximize the following function:

$$Maximize : f(n) = B + F \tag{1}$$

$$B = -\sum_{i=0}^{t-1} \frac{X_i}{T_0} * ln\frac{X_i}{T_0}, X_i = \frac{P_i}{T}, T_0 = \sum_{i=0}^{t-1} X_i \tag{2}$$

$$F = -\sum_{i=t}^{L-1} \frac{X_i}{T_1} * ln\frac{X_i}{T_0}, X_i = \frac{P_i}{T}, T_1 = \sum_{i=t}^{t-1} X_i \tag{3}$$

where P_i determines the number of pixels with a grey value i, and T is the total number of pixels in an image. T_0 and T_1 refer to the respective probabilities of each class. L is the highest value for a pixel in a grey-scale level and equal 255. The previous function was used for finding the threshold value for the bi-level threshold problem. Also, it can be adapted easily for tackling the multi-level threshold problem by redesigning as follows:

$$f(t_0, t_1, t_2, \dots, t_n) = R_0 + R_1 + R_2 + \dots + R_n \tag{4}$$

$$R_0 = -\sum_{i=0}^{t_0-1} \frac{X_i}{T_0} * ln\frac{X_i}{T_0}, X_i = \frac{P_i}{T}, T_0 = \sum_{i=0}^{t_1-1} X_i \tag{5}$$

$$R_1 = -\sum_{i=t_0}^{t_1-1} \frac{X_i}{T_1} * ln\frac{X_i}{T_1}, X_i = \frac{P_i}{T}, T_1 = \sum_{i=t_0}^{t_1-1} X_i \tag{6}$$

$$R_2 = -\sum_{i=t_1}^{t_2-1} \frac{X_i}{T_2} * ln\frac{X_i}{T_2}, X_i = \frac{P_i}{T}, T_2 = \sum_{i=t_1}^{t_2-1} X_i \tag{7}$$

$$R_n = -\sum_{i=t_n}^{L-1} \frac{X_i}{T_n} * ln\frac{X_i}{T_n}, X_i = \frac{P_i}{T}, T_n = \sum_{i=t_n}^{L-1} X_i \tag{8}$$

where n is the number of threshold levels, and t_i is the threshold values such that: $i = 0, 1, 2, \ldots, n$. At the end, our proposed algorithm will work on maximizing Eq. (4) to find the optimal threshold values.

4 Whale optimization algorithm

In WOA, Mirjalili and Lewis (2016) simulates the actions and conducts performed by the humpback whales. The whales surround the victim in a spiral shape swimming up to the surface in a shrinking circle using an astounding feeding method called the bubble-net approach when attacking their victim or prey. WOA simulates this hunting mechanism by making a 50% probability of selecting between a spiral model and a shrinking encircling prey to generate the new position of the current whale. To exchange practically between the spiral model and the shrining encircling mechanism, first, a random number, namely p, is created between 0 and 1 and if this number is less than 0.5, then the encircling mechanism is applied; otherwise; the spiral model is employed. The mathematical formula for the encircling mechanism (exploitation phase) is as follows:

$$\mathbf{S}_i(it+1) = \mathbf{S}^*(it) - \mathbf{A} * \mathbf{D} \tag{9}$$

$$\mathbf{A} = 2 * a * rand - a \tag{10}$$

$$a = 2 - 2 * \frac{it}{t_{maxIter}} \tag{11}$$

$$\mathbf{D} = |\ \mathbf{C} * \mathbf{S}^*(it) - \mathbf{S}_i(it)\ | \tag{12}$$

$$\mathbf{C} = 2 * rand \tag{13}$$

where $\mathbf{S}_i$ is the position of the current i^{th} whale, it is the current iteration, $\mathbf{S}^*$ is the position of the best whale in the population, *rand* is a random number in [0, 1], $t_{maxIter}$ refers to the course of iterations, $\mathbf{D}$ is computed using Eq. (12) which measures the distance between the best-so-far solution, multiplied by a random number C between 0 and 2, and the current i^{th} whale and a is a distance control parameter linearly decreased from 2 to 0. The spiral model tries to mimic the helix-shaped movement of whales, so it is proposed between the position of the victim and the whale. The mathematical model of a spiral shape (exploitation phase) is as follows:

$$\mathbf{S}_i(it+1) = \mathbf{S}^*(it) + \cos(2 * \pi * l) * e^{l*b} * \mathbf{D}' \tag{14}$$

$$\mathbf{D}^{'} = |\ \mathbf{S}^{*}(it) - \mathbf{S}_{i}(it)\ | \tag{15}$$

where $\mathbf{D}^{'}$ indicates the distance between the position vector of prey and i^{th} whale, l is a random number between $[-1, 1]$, b is a constant to describe the logarithmic spiral shape. To search for the prey in another direction in the search area, WOA uses a random whale from the population to update the position of the current whale in the exploration phase. If $\mathbf{A}$ is greater than 1, then the current whale is updated according to a random whale from the population. The mathematical model of the search for the prey (exploration phase) is as follows:

$$\mathbf{S}_{i}(it + 1) = \mathbf{S}_{\mathbf{rand}}(it) - \mathbf{A} * \mathbf{D} \tag{16}$$

$$\mathbf{D} = |\ \mathbf{C} * \mathbf{S}_{\mathbf{rand}}(it) - \mathbf{S}_{i}(it)\ | \tag{17}$$

where $\mathbf{S}_{\mathbf{rand}}$ is a random position vector selected from the current population. The pseudo-code of the standard whale optimization algorithm is described in Algorithm 1.

Algorithm 1 The standard WOA

Initialize the population of whales $S_i (i = 1, 2, 3, \dots, n)$
Evaluate the fitness of each whale
Find the best whale S^*
$it = 1$
while $it < t_{maxIter}$ **do**
  for each i whale **do**
    Update a, A, p, C, and l
    if $p < 0.5$ **then**
      if $|A| < 1$ **then**
        Update $\mathbf{S}_i(it + 1)$ using Eq. 9
      else
        Update $\mathbf{S}_i(it + 1)$ using Eq. 16
      end if
    else
      Update $\mathbf{S}_i(it + 1)$ using Eq. 14
    end if
  end for
  Check the objective value of the whale $\mathbf{S}_i(it + 1)$
  Replacing the best whale S^* with $\mathbf{S}_i(it + 1)$ if better.
  it++
end while

5 The proposed approach

In this section, the improved whale optimization algorithm (IWOA) is adapted for tackling multi-threshold image segmentation problems. IWOA is improved using two strategies to promote its exploration and exploitation capabilities:

– The first strategy is the linearly convergence increasing and local minima avoidance technique (LCMA) that moves the positions of the worst solutions to the direction of the best-so-far solution or within the search space of the problem to prevent stuck into local minima.

– The second strategy is the ranking-based updating method (RUM) to replace the unbeneficial solutions with other better solutions, helping in improving its performance.

The next subsections will illustrate the proposed algorithm in more detail.

5.1 Initialization

In this phase, a population of N whales is randomly generated. The dimension of each whale is initialized randomly within the boundaries of gray levels of the image as illustrated in the following equation:

$$S_{i,j} = H_{min} + rand(0,1) * (H_{max} - H_{min}) \tag{18}$$

where H_{min} and H_{max} is the minimum and maximum of the gray level values in the image histogram, and $rand(0,1)$ is a random number in the range of [0, 1]. The grey-scale level is represented in 8-bit, where the lowest value in decimal is 0 and the highest is $2^8 - 1 = 255$. For representing the positions of the whales within $H_{min} = 0$ and $H_{max} = 255$, Eq. (18) will be used to distribute the position of each whale within this boundary. For example, let's imagine an image with homogenous regions (n) equal to 10. For finding those threshold values that will separate those regions from each other using the WOA, then WOA will spread its solutions within the search space randomly as shown in Fig. 1 that depicts a solution from among all the solutions to illustrate a representation of the solutions to the image segmentation problem for the grey-scale image.

After distributing the solutions within the boundaries of the problem, these values should be transformed into integers because each pixel in the grey image is represented with only 8-bit for an integer value and subsequently each pixel will only load an integer value not decimal. As a result, the values before the dot within Fig. 1 will be used to represent the solution for the image segmentation problem and the numbers after the dot will be truncated as shown in Fig. 2.

Afterward, the integers in Fig. 2 will be arranged as depicted in Fig. 3 and Eq. (4) is called to calculate the quality of those threshold values under Kapur's entropy.

→Threshold level of 10←

5.1	12.5	20.5	100.5	50.5	30.2	150.3	200.1	250.2	80.4

Fig. 1 Depiction of a solution to multilevel thresholding

→Threshold level of 10←

5	12	20	100	50	30	150	200	250	80

Fig. 2 Unordered integer threshold values

→Threshold level of 10←

5	12	20	30	50	80	100	150	200	250

Fig. 3 Ordered integer threshold values

The previous steps will distribute the dimensions (number of threshold values required) of the problem within the search space, convert them into integer values, arrange them, and evaluate them using Eq. (4) will be applied for each solution within the initialization step. After that, the initialization step will terminate and the solution created using WOA within the optimization process will be only converted into an integer, arranged, and evaluated using Eq. (4).

5.2 Linearly convergence increasing and local minima avoidance strategy

We propose a linearly convergence increasing and local minima avoidance strategy (LCMA) to accelerate the convergence speed of the worst solutions toward the best solution and at the same time to avoid the local minima problem that the optimization algorithms may fall into. LCMA updates a number of K worst individuals, or whales for consistency with the proposed algorithm, in the population towards the best solution found so far and randomly within the search space of the problem based on a certain probability known as exploration rate (ER) to avoid falling into local minima. We can calculate K using the following equation:

$$K = N - round\left(\frac{it}{maxIter} * (N - x)\right) \tag{19}$$

where N determines the size of the population, it is the current iteration, $maxIter$ is the maximum number of iterations, and x is a fixed number of the solutions that will be updated within each iteration. *round* is used to round a number to the nearest integer. After calculating the number of worst individuals K, we update each one of the worst individuals $\mathbf{w_j}$ using Eq. (20) to update their positions toward the best solution gradually.

$$\mathbf{w_j} = \mathbf{w_j} + \mathbf{U} * \mathbf{r} * (\mathbf{H_{max}} - \mathbf{H_{min}}) + \mathbf{r_1} * (\mathbf{S}^* - \mathbf{w_j}), j = 1, 2, \dots, K \tag{20}$$

where $\mathbf{w_j}$ refers to the worst solution, and $\mathbf{r}$ is a random numerical vector in the range of [0, 1]. $\mathbf{H_{max}}$ and $\mathbf{H_{min}}$ are two vectors used to contain the upper bound and the lower bound of the search space of the optimization problem, respectively. $\mathbf{U}$ is a binary vector used to determine if the exploration capability will be applied or not, and will be generated according to the following formula:

$$\mathbf{U} = \mathbf{r_2} > ER \tag{21}$$

In Eq. (21), if the current position in $\mathbf{U}$ vector corresponding to a value in $\mathbf{r_2}$ vector is greater than ER then this position will take a value of 1 (which this position will take an exploration capability), otherwise it will take a value 0. Algorithm 2 illustrates the steps of the LCMA technique.

Algorithm 2 LCMA technique

1: Calculate K using Eq. 19.
2: Find the list of solutions that has the worst fitness in the population using quicksort
3: **for** j = 1 to K **do**
4: Update each worst solution $\mathbf{w_j}$ using Eq. 20 in the population
5: **end for**

Typically, at the start, the optimization algorithms give the highest capability for exploration even exploring most of the regions within the search space. This capability may waste most of the iterations within the optimization process without any benefits, although the best current solution may not be a local minima. Subsequently, paying attention to the best-so-far solution will help in reaching the optimal solution in less time. Based on that, we propose this methodology to give the optimization algorithm a high ability on finding a better solution in a reasonable time. On the other side, in some of the meta-heuristic algorithms, its exploration capability is erased at the end of the iterations and subsequently, the possibility of finding a better solution if the current best one is local is impossible. As a result, we support a part within our methodology to dispose of this problem by giving the optimization algorithm ability on searching within the search space of the problem for a better solution. The advantage of LCMA is helping in accelerating the convergence speed toward the best-so-far solution with decreasing falling into the local minima problem.

Our methodology is distinct from the evolutionary population dynamics (EPD) (Saremi et al. 2015) where, in EPD, the worst *n*/2 solutions are removed from the population and added alternatively *n*/2 solutions generated randomly around the best-so-far solution. On the other hand, LCMA will select a number of the worst-so-far solution to move them toward the best-so-far randomly with exploration rate within the search space of the problem based on a certain probability (ER) to avoid stuck into local minima. In addition, this number of the worst selected solution will start with a small number and increases with the iteration until reaching the maximum (all the individuals within the population) at the end of the iteration.

5.3 Ranking -based updating method (RUM)

Recently, a new strategy (Abdel-Basset et al. 2020) known as a ranking strategy has been proposed to replace the unbeneficial solutions with others helping the algorithm in reaching better outcomes. The main obstacle in front of this strategy is the updating method used to generate a new solution in the form that will improve the performance of the proposed algorithm. Therefore, within our work, a new updating method to promote the exploitation

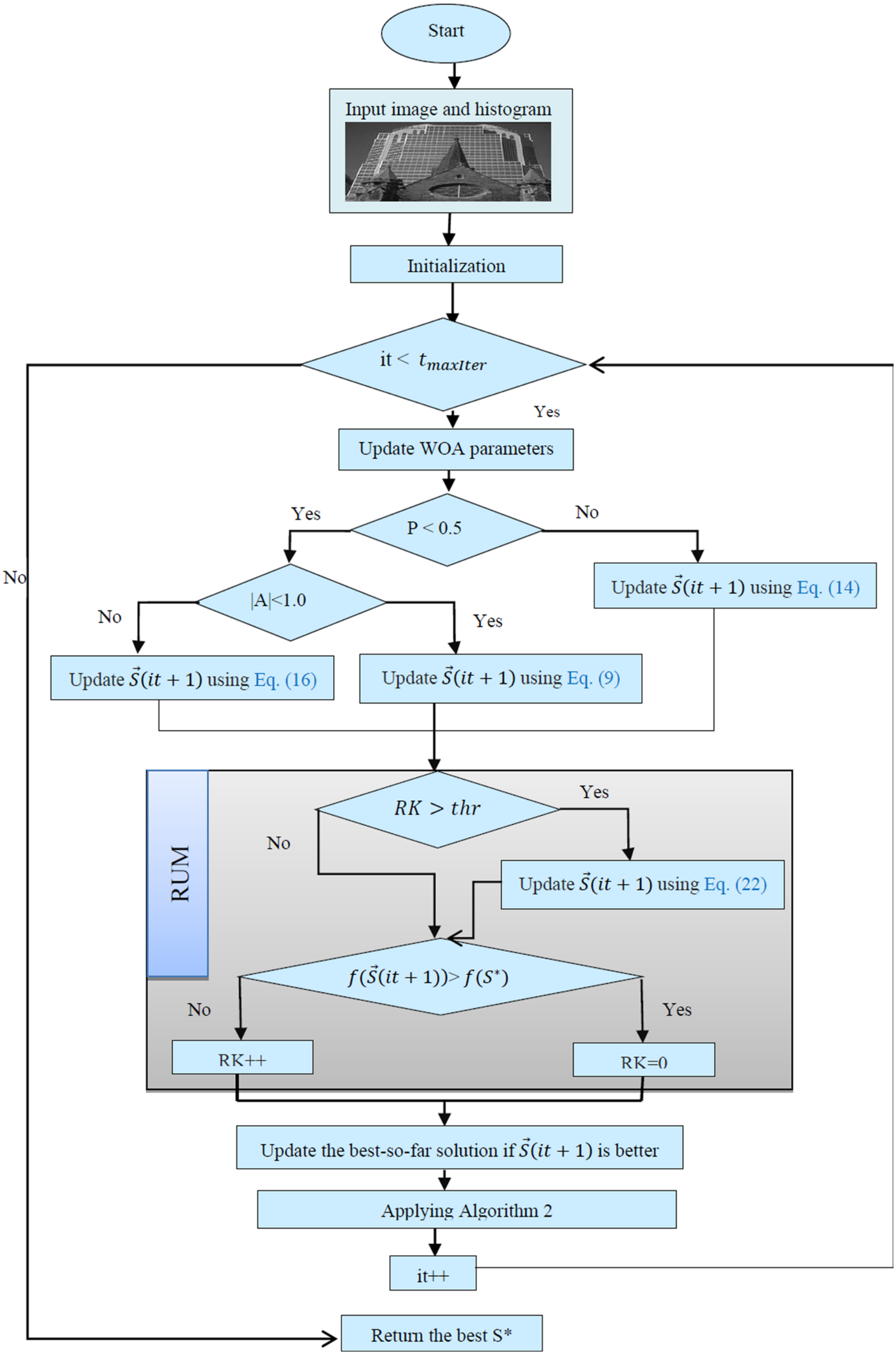

Fig. 4 Flowchart of the proposed algorithm IWOA for Multi-threshold image segmentation problem

capability gradually with the iteration even reaching the maximum at the end of the iteration is proposed. Mathematically, this updating method is formulated as follows:

$$\mathbf{S} = \mathbf{S}^{*} + \mathbf{r} * A * (\mathbf{S_{r1}} - \mathbf{S_{r2}}) \tag{22}$$

Where r_1 and r_2 are the indices of two whales selected randomly from the population. $\mathbf{r}$ is a numerical vector generated randomly between 0 and 1.

5.4 The pseudo-code of IWOA

To evaluate the solutions, we use Eq. (4) as illustrated before in Sect. 3. This function work on finding the homogenous regions based on maximizing the entropy of the histogram. In our proposed algorithm, this function is used as a fitness function to find the optimal threshold values that maximize the variance of an image. The pseudo-code of the proposed algorithm IWOA to solve the multi-thresholding segmentation problem is shown in Algorithm 3 and the same steps are pictured in Fig. 4. In Algorithm 3 shows the pseudo-code of the proposed algorithm IWOA to solve the multi-thresholding segmentation problem. In Algorithm 3, the standard algorithm is integrated with the LCMA strategy to promote its exploitation in addition to avoiding entrapment into local minima as possible. Furthermore, to utilize the whales in the population within the optimization process as much as possible, the RUM is used as an attempt to increase the exploitation capability of the proposed to find a better solution. Broadly speaking, RUM is employed to replace those solutions which spent a consecutive number, namely *Rk*, of the failed attempts exceeding the predefined threshold *thr* recommended 3.

Since the LCMA moves randomly a number of the worst solution toward the best-so-far solution, a large number of the solutions around the best-so-far may be skipped without exploring although of the possibility of finding better solutions within them. Therefore, the RUM is used with the proposed algorithm to explore gradually the solutions around the best-so-far solutions as an attempt to reach better outcomes.

Figure 4 shows the flowchart of the IWOA. At the start, within this figure, the test images and their histogram are inputted to the proposed algorithm; after that, the initialization step is executed to distribute a number of the solutions within the upper and lower bound values of 255 and 0, respectively. Those initialized solutions will be updated by the standard WOA, LCMA, and RUM as depicted in this figure for reaching better fitness values. Finally, the best-so-far solution S^{*} is returned to generate the segmented image using algorithm 4.

Algorithm 3 The proposed IWOA

```
Initialize the population of whales S_i(i = 1, 2, 3, ..., N)
Evaluate the fitness of each whale using Eq. 4
Find the best whale S*
RK: an array of N cells initialized with 0s value
it = 1
while it < t_maxIter do
  for each i whale do
    Update a, A, p, C, and l
    if p < 0.5 then
      if |A| < 1 then
        Update S_i(it + 1) using Eq. 9
      else
        Update S_i(it + 1) using Eq. 16
      end if
    else
      Update S_i(it + 1) using Eq. 14
    end if
    Check the fitness value of the whale S_i(it + 1) using Eq. 4
    if S_i(it + 1) > S* then
      RK_i = 0
    else
      RK_i ++
    end if
    if RK_i > thr then
      Update S_i(it + 1) using Eq. 22
    end if
    Update the best whale S* with S_i(it + 1) if better.
  end for
  Calling Algorithm 2
  it++
end while
Calling algorithm 4 to generate the segmented image.
```

5.5 Our motivations to WOA and segmented image generation algorithm.

At the start, WOA starts with a high exploration capability and this capability gradually reduces with the iteration even fading away after the first half of the iterations. Afterward, the exploitation capability will dominate the whole optimization process to explore most of the regions around the best-so-far solution for finding better if it is not local minima. And this is considered the main advantage of WOA, in addition to the easiness to be understood and implemented, which motivates us to use it. But unfortunately, the WOA suffers from several disadvantages, which are described as follows:

– The high exploration capability at the outset may waste a lot of iterations without any beneficial or utilizing optimally for those the wasted iterations.
– After the first half of the iterations, the exploration capability will be terminated, and subsequently, the possibility of finding a better solution if the current one is local minima is impossible.
– In the second half of the iteration, the exploitation capability will dominate the whole optimization process to explore most of the regions around the best-so-far solution, and

subsequently, a lot of the iterations may be wasted if the current best solution is local minima.

To overcome all those drawbacks, we used LCMA and RUM to help in improving the convergence of the WOA and avoiding stuck into local minima problems within the optimization process. The main advantages of our proposed are listed as:

- Our proposed has a high ability on the exploitation at the outset to increase the convergence toward the best-so-far solution, and high ability on the exploration within the optimization process to help in disposing of local minima problem.
- Utilizing each whale in the population as much as possible for reaching better outcomes.
- Also, it helps in exploiting optimally the individuals of the population within the optimization process.
- Increase the convergence toward the best solution in a reasonable time.
- A small number of parameters for adjustment.

The main drawbacks of our proposed are listed as:

- Picking the value for the ER parameter accurately to adjust the performance of the proposed for reaching a better solution.
- A little expensive for computational cost compared to some other algorithms.

How the segmented image will be generated under the threshold values obtained? Let's suppose that an original image is called A with a number of rows and columns of N and M, respectively. And after finding the optimal threshold values under any threshold level, the segmented image will be generated as shown in algorithm 4.

Algorithm 4 segmented image generation steps (GSI)

```
B: is a matrix of N * M to contain the pixels of the segmented image.
W* = [0 S* 255].
for i = 0 to N do
   for j = 0 to M do
      for m = 0 to t-1 do // number of threshold values obtained
         if A(i,j) ⩾ W*_m && A(i,j) ⩽ W*_{m+1} then
            B(i,j) = W*_m;
         end if
      end for
   end for
end for
Return B;
```

5.6 Time complexity for the pseudo-code of IWOA

To show the speedup of the proposed algorithm, in this section, the time complexity in big-O will be designed to see that. At the outset, the main factors that especially affect the speedup of the proposed algorithm are:

– The population size: N.
– The threshold level: n
– The maximum iteration: $t_{maxIter}$.
– The time complexity of algorithm 2.

In regards to the time complexity formula of the proposed, it is formulated as follows:

$$T(IWOA) = T(WOA) + T(LCMA) \tag{23}$$

Where, the standard WOA is mainly relied only on the former first three factors and that is aggregated in big-O according to algorithm 3 as follows:

$$T(WOA) = O(t_{maxIter}.nN) \tag{24}$$

Regarding the running time of the LCMA, it also depends on the previous four factors with exception of N, which is replaced by the number of worst whales K extracted using the Quicksort algorithm. Since the Quicksort is utilized, its time complexity is of $O(N^2)$ in the worst case for iteration (Xiang 2011). In general, the time complexity of the LCMA is formulated as follows:

$$T(LCMA) = O(Qicksort) + O(repalcingtheworstwhalesk) \tag{25}$$

The time complexity of the quick sort for all iterations is of $O(N^2 t_{maxIter})$ in the worst case, meanwhile, the time complexity of replaing the worst whale is of $O(Knt_{maxIter})$. By compensating in Eq. (25), the time complexity of the LCMA strategy is as follows:

$$T(LCMA) = O(N^2 t_{maxIter}) + O(Knt_{maxIter}) \tag{26}$$

From Eq. (26), the expression that has the highest growth rate is of $O(N^2 t_{maxIter})$. Therefore, the time complexity of the LCMA strategy in the worst case is of $O(N^2 t_{maxIter})$. Likewise, for Eq. (22), that is extended as follows:

$$T(IWOA) = O(t_{maxIter} nN) + O(N^2 t_{maxIter}) \tag{27}$$

From Eq. (27), in final. The time complexity of the IWOA in the worst case is of $O(N^2 t_{maxIter})$.

6 Experiments and discussion

Our experimental studies are performed on a desktop computer using Windows 7 ultimate platform with a 32-bit operating system, Intel Core i3-2330M CPU @ 2.20 GHz, and 1 GB of RAM. The proposed algorithm is tested using low memory capacity to validate working under the most constraint conditions. We use the Java programming language for implementing all algorithms used in our comparisons. In this section, we concern with illustrating the results of our experiments. This section organized as follows:

– Section 6.1 describes the test images used in our experiments.
– Section 6.2 shows the experimental Settings.
– Section 6.3 demonstrates valuation Metrics.
– Section 6.4 compares the performance Evaluation of IWOA and WOA.

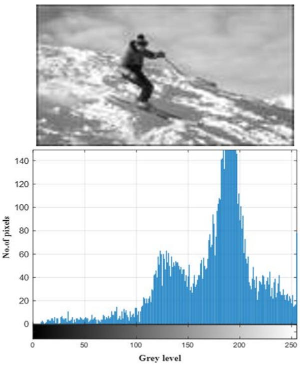

(a) 61060 original image

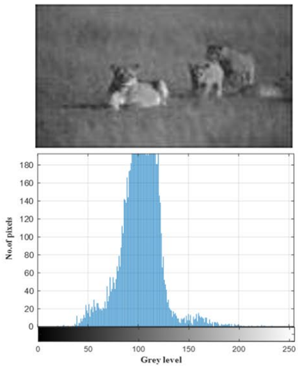

(b) 105053 original image

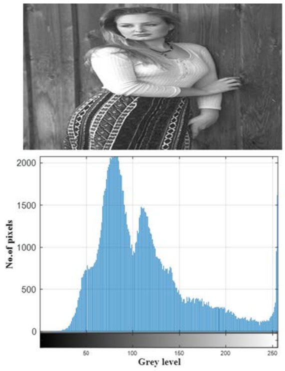

(c) 181079 original image

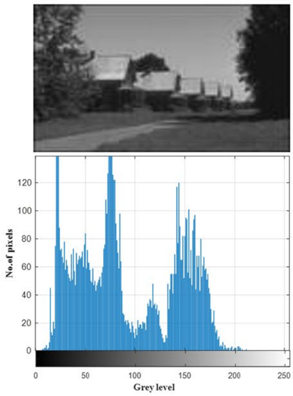

(d) 232038 original image

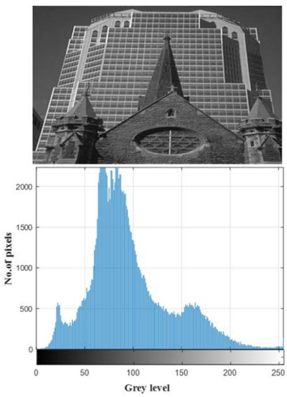

(e) 277095 original image

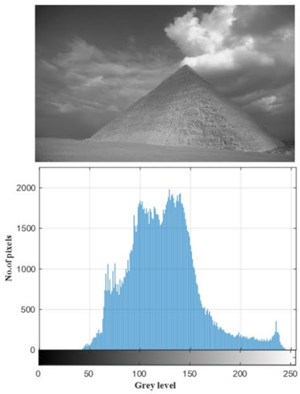

(f) 299091 original image

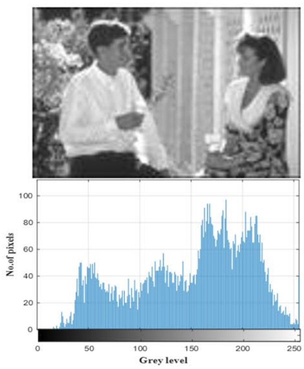

(g) 157055 original image

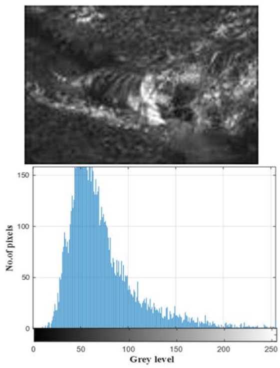

(h) 108070 original image

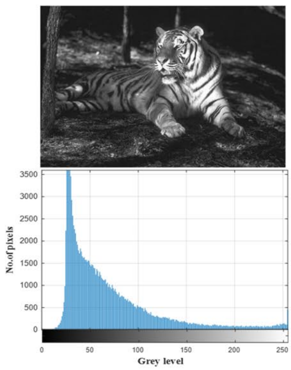

(i) 108082 original image

Fig. 5 Description of the original images and their histograms

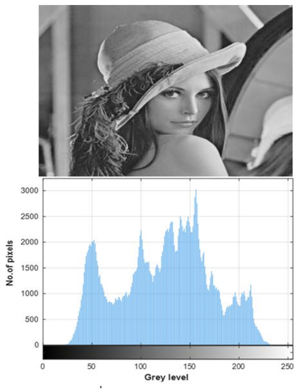

(a) Lena original image

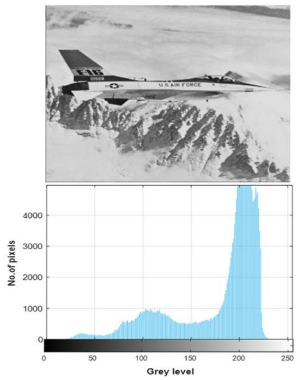

(b) airplane original image

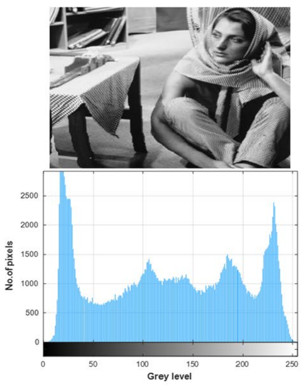

(c) Barbara original image

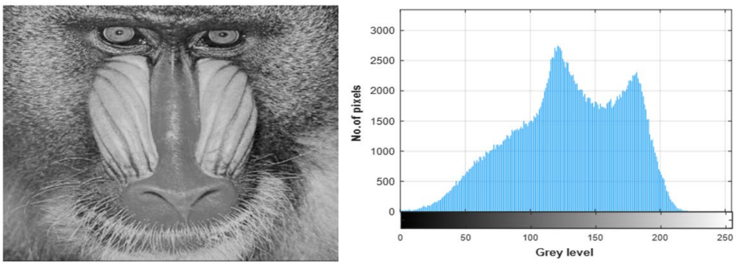

(d) Mandrill original image

Fig. 6 Description of the original images and their histograms

- Section 6.5 investigates the performance Evaluation of our proposed algorithm with the others.
- Section 6.6 displays the segmented Images produced by IWOA.
- Section 6.7 conducts the Wilcoxon rank-sum test.

6.1 Test images description

The performance of our proposed algorithm is evaluated on nine test images taken from the Berkeley Segmentation Dataset (BSDS500), and the identifiers (ID) of those images are 61060, 105053, 181079, 232038, 277095, 299091, 157055, 108070, and 108082, in addition to four common test images: Mandrill, Lena, Barbara, and airplane. We used 13 test images in our paper in the same range where the researches in the literature used, for example, whale optimization algorithm (Abd El Aziz et al. 2017) was validated on eight test images, equilibrium optimizer for multi-level thresholding image segmentation used seven test images (Abdel-Basset et al. 2021), and Multi-Level Image Thresholding Based on Modified Spherical Search Optimizer and Fuzzy Entropy Segmentation (Naji Alwerfali

Table 2 Parameter setting for the proposed IWOA

Parameter	Value
Number of runs	30
Population size	30
The maximum number of iterations	150
X (the number of the redirected particles)	4
ER	0.99
thr	3

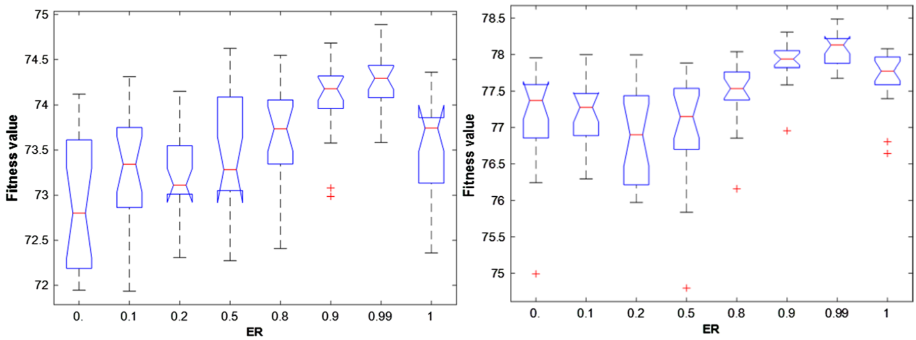

(a) Observing under t=40, image ID=61060 **(b)** Observing under t=40, image ID=105053

Fig. 7 Depiction of the Boxplot for the outcomes obtained under different value for ER parameter

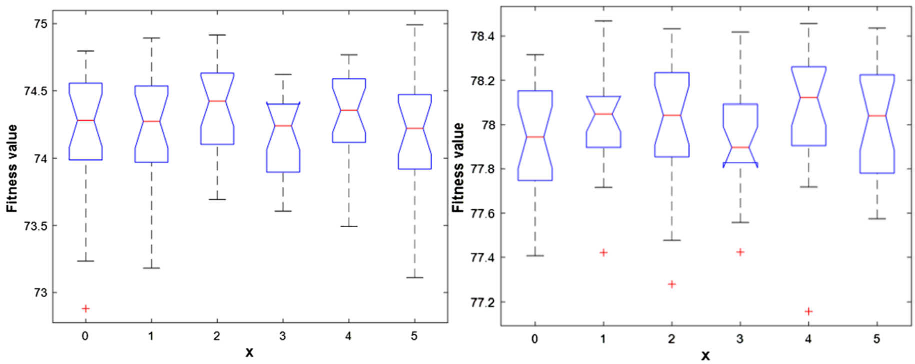

(a) Observing under t=40, image ID=61060 **(b)** Observing under t=40, image ID=105053

Fig. 8 Depiction of the Boxplot for the outcomes obtained under different values for X parameter

et al. 2020) used ten test images. Figures 5, 6 depicts each original image out of the 13 test images and its histogram.

6.2 Parameter settings

Our proposed algorithm is compared with Sine cosine Algorithm (SCA) (Mirjalili 2016), Firefly Algorithm (FFA) (Erdmann et al. 2015), Flower Pollination Algorithm (FPA) (Yang 2012), and standard whale optimization algorithm (Abd El Aziz et al. 2017), L-SHADE (Brest et al. 2016), improved marine predators algorithm (IMPA)(Abdel-Basset et al. 2020), equilibrium optimizer (EO) (Abdel-Basset et al. 2021), crow search algorithm (CSA) (Moses et al. 2019), hybrid WOA (WOA-DE) (Lang and Jia 2019), and salp swarm algorithm (SSA) (Wang et al. 2020). The algorithm parameters are selected based on the standard for these parameters. Also, for a fair comparison, an equal number of function evaluations used with a maximum number of iterations equal 150 and population members set to 30. Additionally, each algorithm runs 30 independently times. Table 2 summarizes the values of the IWOA parameters.

There are two parameters: *ER* and *X* in our proposed algorithm needed to be pick accurately for exploiting optimally the performance of our proposed algorithm. Therefore, extensive experiments are performed to extract the best value for those parameters, all those experiments are demonstrated in Figs. 7 and 8 for *ER* and *X* parameters, respectively. First, let's move toward Fig. 7 that depicts the results of our experiments for extracting the best value of the ER parameter. This figure shows the results obtained on two images: 61060 and 105053 with threshold level 40. And inspecting this figure tells us that the best value for ER is 0.99 where it could outperform all the others in the lowest, Quartile-1 (Q_1), Quartile-2 (Q_2), Quartile-3 (Q_3), and the highest values over two images.

Concerning *X* parameter, an experiment with different values for this parameter involving: 0, 1, 2, 3, 4, and 5 is conducted to extract the best one for this parameter and its results are pictured in Fig. 8 that shows that the best value obtained on two images: 61060 and 105053 with threshold level 40 was by a value of 4, but also for 61060 a value of 2 was competitive with 4. Generally, within our experiments, we used a value of 4 for *X* parameter. Regarding *thr*, *it* is set to as recommended in (Abdel-Basset et al. 2021)

6.3 Evaluation Metrics

We use six criteria to evaluate the performance of the algorithms, including CPU time, fitness values, Standard Deviation (STD), Peak Signal to Noise Ratio (PSNR), Universal Quality Index (UQI), and Structured Similarity Index Metric (SSIM). We will explain these criteria as follows:

- The CPU time is used to calculate the time in seconds taken by each algorithm.
- The fitness function is computed using the Kapur's entropy mentioned above.
- The STD measures the variation and the dispersion of the data of a given algorithm.
- The PSNR (Hore and Ziou 2010) metric measures the quality of the segmented images defined by the following formula:

$$PSNR = 10\log_{10}\left(\frac{255^2}{MSE}\right) \tag{28}$$

where 255 determines the maximum pixel value of an image when we represent a pixel in 8 bits, such that: $2^8 - 1 = 255$. MSE is the mean squared error and is calculated as follows:

$$MSE = \frac{\sum_{i=1}^{M} \sum_{j=1}^{N} \mid O(i,j) - S(i,j) \mid}{M * N} \tag{29}$$

where $O(i, j)$, $S(i, j)$ represent the original and segmented images, respectively. PSNR is inversely proportional to MSE.

– The SSIM (Hore and Ziou 2010) metric calculates the difference between the structure of the segmented and original image. The mathematical formula of SSIM is defined as follows:

$$SSIM(O,S) = \frac{(2\mu_o\mu_s + a)(2\sigma_{os} + b)}{(\mu_o^2 + \mu_s^2 + a)(\sigma_o^2 + \sigma_s^2 + b)} \tag{30}$$

where μ_0 and μ_s defined the average intensity for both original and segmented images, respectively. σ_0 and σ_s refers to the standard deviation of the original and segmented image, also, σ_{0s} stands for the covariance between them. The constant values a and b set to 0.001 and 0.003, respectively.

– UQI (Egiazarian et al. 2006) is another metric utilized to determine the quality of the segmented image compared to the original one based on three factors: loss of correlation, brightness, and contrast distortion. Mathematically, this model is formulated as follows:

$$UQI(O,S) = \frac{4\sigma_{os}\mu_o\mu_s}{(\mu_o^2 + \mu_s^2)(\sigma_o^2 + \sigma_s^2)} \tag{31}$$

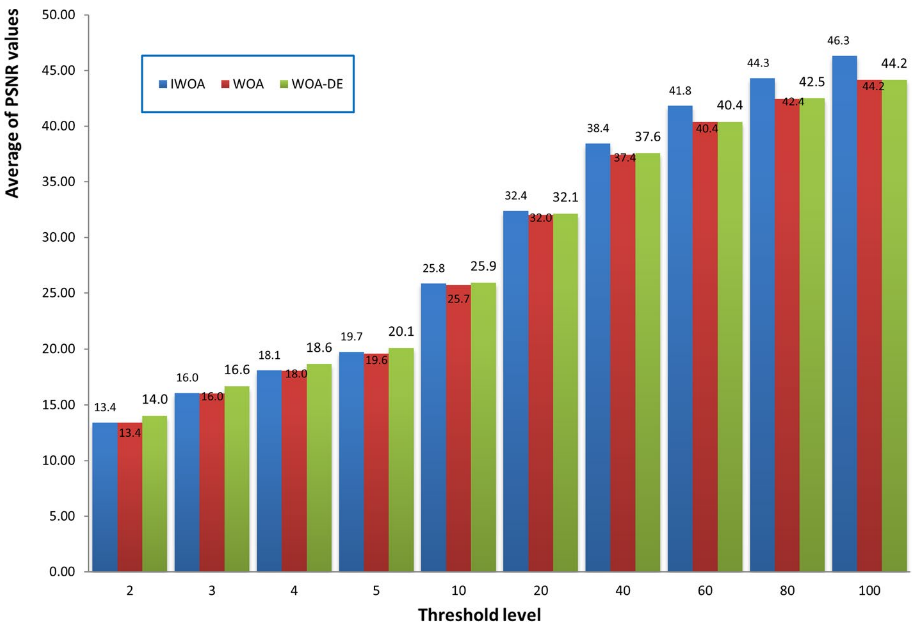

Fig. 9 Comparison between IWOA, WOA, and WOA-DE based on PSNR

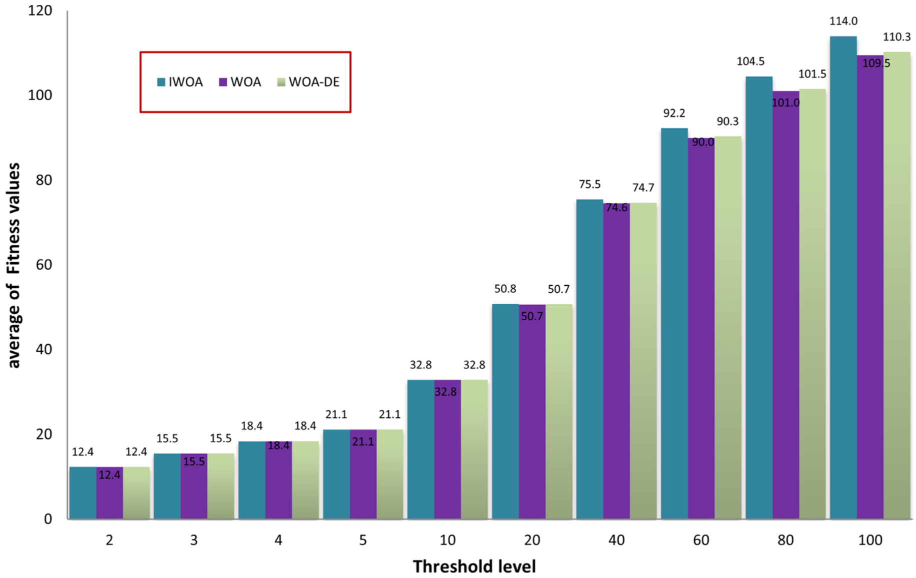

Fig. 10 Comparison between IWOA, WOA, and WOA-DE based on fitness values

The higher value of PNSR and SSIM indicate better performance. PSNR metric work on finding the ratio of the error between the original and the segmented images and don't focus on the structure of the image after the segmentation on the correlation, luminance distortion, and contrast distortion that specifies the quality of the segmented images. As a result, SSIM is used to pay attention to measure the difference between the structures of the original image and segmented based on the following three factors: loss of correlation, luminance distortion, and contrast distortion between the original and segmented images.

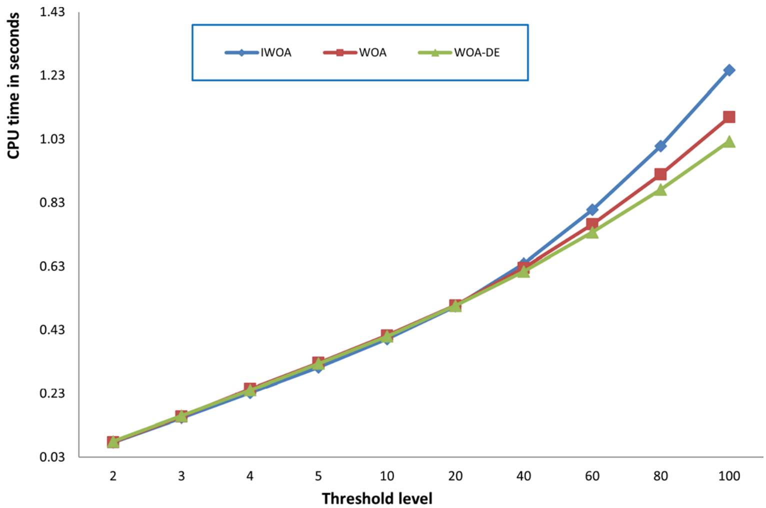

Fig. 11 Average CPU time values on each threshold level

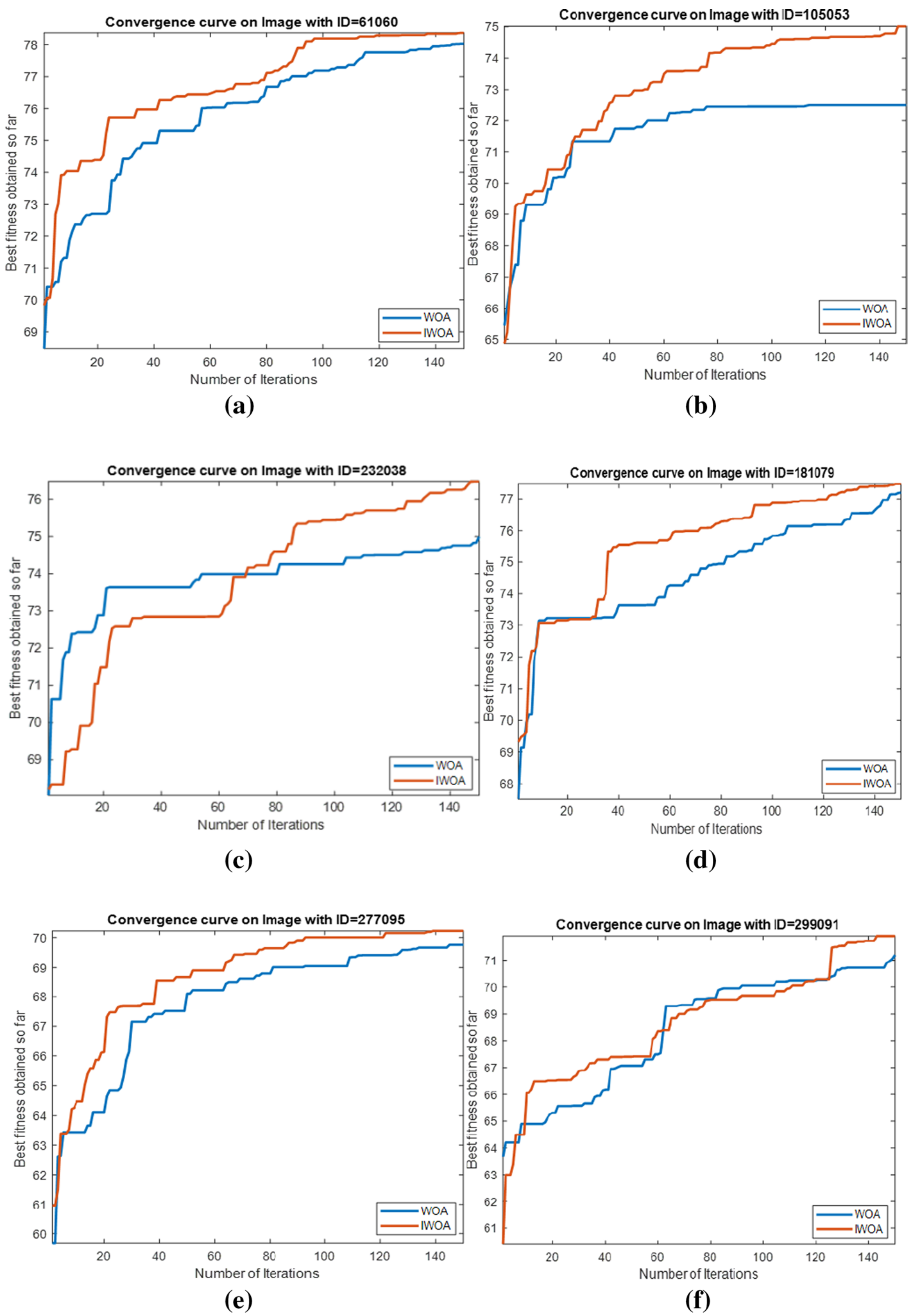

Fig. 12 Comparison between IWOA and WOA under convergence curve obtained by each one on each test image under t=40

6.4 The performance evaluation of IWOA, WOA, and WOA-DE

Here, we seek to prove the efficacy of the proposed algorithm in comparison with the standard WOA and WOA-DE. We are interested in studying the effect of using the LCMA technique on the performance of the proposed algorithm. Figure 9 compares the three algorithms using different threshold values, including 2, 3, 4, 5, 10, 40, 60, 80, and 100. The figure shows the average PSNR values obtained by running each algorithm 30 times for all the test images for each threshold level. By observing the figure, we can see that WOA-DE reaches better PSNR for threshold levels of 2, 3, 4, 5, and 10, higher than that, the proposed algorithm could fulfill PSNR values significantly-better than the others. Consequently, IWOA obtains a higher quality segmented image than the other two WOA variants when increasing the threshold levels. Another comparison is presented in Fig. 10 based on the average fitness values of Kapur's entropy. We use different threshold values, including 2, 3, 4, 5, 10, 20, 40, 60, 80, and 100, to show the consistency of the proposed algorithm within various threshold levels. At first, we obtain the fitness values of running each algorithm 30 times on a given threshold level. Then, we compute the average fitness value for each threshold level as the summation of the fitness values through 30 runs divided by 30. The figure shows that IWOA succeeds in obtaining better fitness values compared to WOA and WOA-DE for all different threshold levels higher than 10 and equal with the rest. In Fig. 11, unfortunately, IWOA couldn't outperform the WOA and WOA-DE in CPU time for threshold levels higher than 40. However, the proposed algorithm is better as it outperforms WOA based on PSNR and fitness values.

Regarding evaluating the convergence obtained by IWOA and WOA within the optimization process, Figure 12 is introduced to show that on all test images with a threshold level (t) of 40. We selected this threshold level to measure how far each algorithm could perform better with a high threshold level. After inspecting this figure, we found that IWOA could outperform WOA in the convergence within the starting of the optimization process for images: 61060, 105053, 181079, 277095, and 299091 and its superiority move on until the ending. However, for the other images, the convergence curve for WOA appears to be the best at the starting of the optimization process, afterward, this appearance deteriorates due to the local minima problem and our proposed dramatically outperforms.

6.5 The performance evaluation of the proposed algorithm and other algorithms

Tables 3, 4, 5 presents a comparison among the algorithms based on the average PSNR values using different Threshold levels (n), including 2-n, 3-n, 4-n,5-n,10-n,20-n,30-n, 40-n, 60-n,80-n, and 100-n. For each threshold level, we compute the average PSNR as follows:

$$PSNR_{Avg} = \frac{\sum_{i=1}^{R} PSNR_i}{R}, R = 1, \ldots, 30 \tag{32}$$

$PSNR_{Avg}$ is the summation of the PSNR computed for each run of an algorithm for a given threshold level divided by the number of running the algorithm. R is the number of independent runs for the algorithms, which is 30. Based on the results introduced in the table, the proposed algorithm can outperform the other algorithms in the PSNR metric. For the small threshold levels, we can see that IWOA could be competitive and superior to the others in most of the test images. For the higher threshold values, the performance of the other algorithms is degraded, while IWOA gets the maximum average PSNR for all the test

Table 3 The PSNR values obtained by each algorithm on different threshold levels

ID	Algorithm	Threshold level (n)									
		2-n	3-n	4-n	5-n	10-n	20-n	40-n	60-n	80-n	100-n
61060	IWOA	**16.2867**	**16.7692**	**18.7869**	20.2126	**25.5552**	**31.5556**	**37.6849**	**41.4087**	**43.9277**	**45.7956**
	IMPA (Abdel-Basset et al. 2020)	**16.2867**	16.6497	**18.7869**	**20.6893**	25.5117	30.9022	35.6584	38.2204	40.3062	42.026
	FFA (Erdmann et al. 2015)	**16.2867**	16.5289	18.7641	20.1954	25.1383	29.8495	32.9637	35.2004	37.0466	38.3628
	SCA (Mirjalili 2016)	16.2624	16.5125	18.528	20.6307	25.1069	29.8977	35.0462	37.6503	39.7634	41.5877
	FPA(Yang 2012)	16.2855	16.4567	18.5627	20.5322	24.7915	29.0752	34.3168	36.9882	39.1574	41.2035
	L-SHADE(Brest et al. 2016)	15.7974	16.1315	18.1156	19.4022	23.7514	28.5646	33.5875	35.8807	38.6393	40.8016
	SSA (Wang et al. 2020)	**16.2867**	16.617	18.7624	20.3786	24.5493	29.4472	32.431	35.6409	37.4665	38.9306
	EO(Abdel-Basset et al. 2021)	**16.2867**	16.7095	**18.7869**	20.2083	25.0504	29.7666	33.1060	35.3548	37.1199	38.9897
	CSA(Moses et al. 2019)	16.2795	16.4914	18.7005	20.6590	25.0777	29.7559	34.2771	37.0703	39.5528	41.3172
105053	IWOA	8.1763	**17.4895**	**17.7293**	20.7808	**26.6813**	32.7199	39.1301	**42.3156**	**44.6779**	**46.881**
	IMPA(Abdel-Basset et al. 2020)	8.1763	17.4895	17.4435	21.0702	26.2227	**33.191**	**39.2632**	41.6234	43.8625	45.9313
	FFA (Erdmann et al. 2015)	8.1763	17.4753	17.6355	21.3868	27.0934	32.8384	37.7095	40.9477	42.5877	44.4127
	SCA (Mirjalili 2016)	8.1633	17.3352	17.341	**21.4962**	25.5527	30.0635	35.0526	38.3385	40.5995	42.028
	FPA(Yang 2012)	8.174	17.3413	17.3105	21.3455	25.6217	30.1868	35.4511	38.3075	40.0721	42.6076
	L-SHADE(Brest et al. 2016)	**9.6425**	16.1628	17.5898	19.2213	23.7277	28.802	34.3476	37.5381	39.6678	42.1126
	SSA (Wang et al. 2020)	8.1763	17.4679	17.407	20.94	27.0642	32.8371	37.7193	40.7466	43.158	44.9611
	EO(Abdel-Basset et al. 2021)	9.4004	**17.4895**	18.1580	**21.7813**	26.6968	**33.3049**	**39.5285**	**42.8861**	**45.2782**	46.3812
	CSA(Moses et al. 2019)	8.1695	17.3392	17.2921	21.5001	25.8554	30.9389	35.9129	39.2477	41.1463	43.2806

Table 3 (continued)

ID	Algorithm	Threshold level (n)									
		2-n	3-n	4-n	5-n	10-n	20-n	40-n	60-n	80-n	100-n
181079	IWOA	**10.9408**	13.5952	18.6509	19.7918	26.1093	**31.742**	**37.8592**	**41.5339**	**43.7337**	**45.9791**
	IMPA(Abdel-Basset et al. 2020)	**10.9408**	13.5952	18.6295	19.8006	**26.1567**	31.7284	37.4946	39.9403	41.6452	42.9932
	FFA (Erdmann et al. 2015)	**10.9408**	13.5956	**18.7702**	19.8336	26.0867	30.7462	34.7174	36.4639	39.3715	40.7335
	SCA (Mirjalili 2016)	10.9647	13.6067	18.5867	19.6452	25.1353	29.5348	34.453	37.5382	39.8938	41.1671
	FPA(Yang 2012)	10.9408	13.5314	18.6755	19.7329	24.7949	29.4295	34.3434	37.1452	39.9103	41.5033
	L-SHADE(Brest et al. 2016)	11.3971	**15.075**	17.0602	19.0854	23.5204	28.6653	34.0922	36.5777	39.0134	41.2603
	SSA (Wang et al. 2020)	10.9408	13.596	18.7222	**19.8396**	26.1203	30.9164	34.8317	37.5808	38.8031	40.7615
	EO(Abdel-Basset et al. 2021)	10.9408	13.8211	18.7563	19.8096	26.0668	31.5504	36.1967	38.7301	40.5557	41.9747
	CSA(Moses et al. 2019)	10.9489	13.6335	18.6553	19.7121	25.3675	29.9050	35.0332	38.2055	39.8197	41.8183
232038	IWOA	**13.0048**	15.1266	18.1124	**19.8585**	24.2759	**31.987**	**38.0154**	**41.3027**	**43.691**	**45.7513**
	IMPA(Abdel-Basset et al. 2020)	**13.0048**	15.1266	18.8365	19.7179	**24.4223**	31.7808	37.5034	40.6755	42.4778	44.4932
	FFA (Erdmann et al. 2015)	**13.0048**	15.1302	18.9594	20.0016	25.0449	31.0259	35.9598	38.979	41.2838	43.1382
	SCA (Mirjalili 2016)	12.9986	15.1485	19.0294	19.7184	23.7883	29.3839	34.9091	37.2016	39.8539	41.5944
	FPA(Yang 2012)	13.004	15.1197	**19.385**	19.547	24.3978	29.7331	34.3111	37.7972	39.6273	41.4956
	L-SHADE(Brest et al. 2016)	13.004	**15.6361**	17.4787	18.6656	23.2296	27.4646	33.3554	36.6544	39.1189	40.7351
	SSA (Wang et al. 2020)	13.0048	15.1287	18.945	19.7159	24.9574	31.3648	36.4699	39.5262	41.7867	42.8996
	EO(Abdel-Basset et al. 2021)	**13.0048**	15.1266	19.2749	19.7192	**25.0847**	31.6771	37.4857	41.1474	43.1810	44.6525
	CSA(Moses et al. 2019)	13.0030	15.1346	19.3847	19.6840	24.1848	29.5117	34.9319	37.7080	40.2279	42.1482

Table 3 (continued)

ID	Algorithm	Threshold level (n)									
		2-n	3-n	4-n	5-n	10-n	20-n	40-n	60-n	80-n	100-n
277095	IWOA	**17.2331**	**19.5955**	20.0944	22.2815	27.9087	34.1189	**40.4472**	**44.0415**	**46.5726**	**48.872**
	IMPA(Abdel-Basset et al. 2020)	**17.2331**	19.3947	20.0944	22.3408	28.0279	34.3134	40.3225	43.4826	44.9598	46.6855
	FFA (Erdmann et al. 2015)	**17.2331**	19.4469	20.3817	22.3397	28.0926	**34.372**	39.6988	41.8509	43.2272	44.6291
	SCA (Mirjalili 2016)	17.2592	19.4005	20.1383	22.0145	26.9085	31.9687	36.0582	39.435	42.0242	43.736
	FPA(Yang 2012)	17.2462	19.3746	20.339	22.1086	26.469	30.7319	35.1382	38.7162	41.2978	42.7415
	L-SHADE(Brest et al. 2016)	16.6452	18.3082	19.6956	20.6929	24.0195	29.1134	33.9374	37.4709	39.4088	41.6076
	SSA (Wang et al. 2020)	**17.2331**	19.5076	**20.3945**	**22.3716**	**28.1538**	34.2436	39.4361	41.4285	43.6577	45.6107
	EO(Abdel-Basset et al. 2021)	**17.2331**	19.5318	20.0944	22.2582	27.8796	34.0662	39.5489	42.6040	44.9147	46.7984
	CSA(Moses et al. 2019)	17.2495	19.5695	20.3456	22.0283	27.0782	31.2230	36.4326	39.4172	42.0179	43.4224

Bold values indicate the best value

Table 4 The PSNR values obtained by each algorithm on different threshold levels

ID	Algorithm	Threshold level (n)									
		2-n	3-n	4-n	5-n	10-n	20-n	40-n	60-n	80-n	100-n
299091	IWOA	**12.7506**	**14.7732**	17.4413	19.4405	26.649	33.2916	39.4496	**42.9397**	**45.4949**	**47.2838**
	IMPA(Abdel-Basset et al. 2020)	**12.7506**	**14.7732**	17.4413	18.5549	26.7035	**33.3705**	**39.9062**	42.8988	44.9928	46.5953
	FFA (Erdmann et al. 2015)	**12.7506**	**14.7732**	**17.5053**	**20.8595**	27.2694	33.0254	37.5475	40.406	42.5489	43.7756
	SCA (Mirjalili 2016)	12.6001	14.6274	17.5049	19.6115	25.8008	30.2924	35.3947	38.2696	40.6356	42.4988
	FPA(Yang 2012)	12.7343	14.6982	17.5	19.1003	26.0155	30.5486	35.0727	38.1241	40.4536	42.9055
	L-SHADE(Brest et al. 2016)	12.7018	14.3751	16.9103	19.2296	24.4079	29.2449	34.1894	37.4026	39.5417	41.8211
	SSA (Wang et al. 2020)	**12.7506**	**14.7732**	17.4821	19.3247	**27.3287**	32.7439	37.8646	40.2891	42.6772	44.775
	EO(Abdel-Basset et al. 2021)	12.7506	14.7732	17.4413	19.4697	27.3109	33.5670	38.3367	41.4319	43.7787	45.0486
	CSA(Moses et al. 2019)	12.7343	14.7640	17.4171	19.6498	26.1747	31.1799	36.1748	39.0938	41.5331	43.4786
157055	IWOA	**14.8685**	16.82	18.7981	19.4275	**26.274**	31.916	**38.0734**	**41.5321**	**43.9867**	**45.9721**
	IMPA(Abdel-Basset et al. 2020)	**14.8685**	16.8202	18.8129	19.4275	26.1992	**31.9554**	37.4332	40.7193	42.6234	44.3435
	FFA (Erdmann et al. 2015)	**14.8685**	16.8252	**18.827**	**19.4485**	26.2039	31.0721	35.6588	38.2036	40.3306	41.8274
	SCA (Mirjalili 2016)	14.8616	**16.8316**	18.7873	19.2676	25.0025	29.7745	34.6014	37.391	39.77	41.5039
	FPA(Yang 2012)	14.8641	16.8188	18.4205	19.3255	24.8499	29.2591	34.2189	37.2836	39.6526	41.4933
	L-SHADE(Brest et al. 2016)	14.637	16.4629	17.7539	18.7346	23.3999	28.056	33.2929	36.4933	39.0554	40.9173
	SSA (Wang et al. 2020)	**14.8685**	16.8223	18.8185	19.4271	26.1326	31.041	35.8873	38.0579	39.9067	41.7728
	EO(Abdel-Basset et al. 2021)	**14.8685**	16.8190	18.8086	19.4363	26.2407	31.2912	36.0481	38.4696	40.5889	42.1586
	CSA(Moses et al. 2019)	14.8652	16.8220	18.6925	19.3459	25.3089	29.9455	34.8648	37.8973	40.0332	41.9029

Table 4 (continued)

ID	Algorithm	Threshold level (n)									
		2-n	3-n	4-n	5-n	10-n	20-n	40-n	60-n	80-n	100-n
108070	IWOA	**12.8967**	**14.2363**	15.7475	17.7623	**25.9934**	**32.5243**	**38.4528**	**41.1617**	**43.6999**	**45.4801**
	IMPA(Abdel-Basset et al. 2020)	**12.8967**	**14.2363**	15.7304	17.0121	25.1283	32.5107	38.0452	40.4146	42.2708	44.3453
	FFA (Erdmann et al. 2015)	**12.8967**	**14.2363**	15.833	17.8724	24.7973	32.1232	36.7794	39.4306	41.6915	42.5833
	SCA (Mirjalili 2016)	12.8869	14.3027	15.5702	**17.9583**	24.9282	30.1214	34.2607	37.4506	39.7926	41.2647
	FPA(Yang 2012)	12.8965	14.2737	15.6903	17.7294	24.9322	29.9455	35.0972	37.6076	39.905	42.0306
	L-SHADE(Brest et al. 2016)	12.7868	14.1071	**16.2789**	17.7593	23.7576	29.0393	33.9972	36.9642	39.1351	41.158
	SSA (Wang et al. 2020)	**12.8967**	**14.2363**	15.7986	17.758	24.8294	32.3343	37.0911	39.0282	41.5582	42.2324
	EO(Abdel-Basset et al. 2021)	12.8965	14.2737	15.6903	17.7294	24.9322	29.9455	35.0972	37.6076	39.9050	42.0306
	CSA(Moses et al. 2019)	12.7868	14.1071	**16.2789**	17.7593	23.7576	29.0393	33.9972	36.9642	39.1351	41.1580
108082	IWOA	**14.5453**	16.0075	17.1678	18.0151	**23.1348**	**31.4783**	**36.7836**	**40.1501**	**42.9475**	**44.8308**
	IMPA(Abdel-Basset et al. 2020)	**14.5423**	**16.0369**	17.1311	17.8325	21.7034	30.9698	36.2668	39.3682	41.373	43.4287
	FFA (Erdmann et al. 2015)	**14.5423**	16.0368	17.197	18.1359	22.7504	30.7971	34.7235	38.0501	39.706	42.2618
	SCA (Mirjalili 2016)	14.534	15.9818	**17.2315**	17.9926	22.7623	29.145	33.9605	37.0217	39.8852	41.1458
	FPA(Yang 2012)	14.5423	15.9806	17.1285	17.924	22.792	29.495	33.6834	37.5135	39.2886	41.6687
	L-SHADE(Brest et al. 2016)	14.5417	16.0231	16.9894	18.1094	22.606	27.9576	33.2503	36.4203	38.3674	40.6714
	SSA (Wang et al. 2020)	**14.5423**	16.0259	17.196	**18.1525**	22.1649	31.0065	35.359	38.3042	40.0028	41.9553
	EO(Abdel-Basset et al. 2021)	14.5453	16.0369	17.1931	18.0947	**23.5194**	31.0019	35.9745	39.5162	41.5182	42.6250
	CSA(Moses et al. 2019)	**14.5489**	15.9921	17.2301	18.0076	22.2066	29.5041	34.6427	37.7308	40.2057	42.3192

Bold values indicate the best value

Table 5 The PSNR values obtained by each algorithm on different threshold levels

ID	Algorithm	Threshold level (n)									
		2-n	3-n	4-n	5-n	10-n	20-n	40-n	60-n	80-n	100-n
Barbara	IWOA	14.9240	17.3240	19.0009	**20.6601**	**25.1294**	**31.2820**	**37.3790**	**40.9505**	**43.4813**	**45.0693**
	IMPA	14.9240	17.3240	19.0009	20.6529	25.0946	30.8266	37.3247	40.5081	42.3595	44.1365
	FFA	14.9240	**17.3243**	18.9989	20.6374	24.9916	30.9267	36.3082	39.1633	40.8988	42.4291
	SCA	**14.9343**	17.3251	18.9987	20.6534	24.6423	28.9304	33.6535	37.4021	39.3181	41.1608
	FPA	14.9253	17.3223	18.9569	20.5960	24.3680	28.9210	34.0246	36.9185	39.2672	41.2625
	L-SHADE	14.8961	17.2009	18.7727	20.2293	23.9052	28.4566	33.3502	36.7070	38.8824	40.6336
	SSA	14.9240	17.3245	18.9967	20.6365	24.9814	30.9075	35.8686	38.6984	41.1878	42.6449
	EO	14.9240	17.3240	19.0009	20.6494	25.1599	30.7916	35.7825	38.7773	41.0402	42.7376
	CSA	14.9249	17.3239	**19.0022**	20.6149	24.5367	29.1929	34.4222	37.6804	39.9503	41.6369
Airplane	IWOA	16.0751	18.8125	**20.4488**	21.3370	**27.3730**	**32.3476**	**38.4140**	41.9920	**45.0835**	**46.6236**
	IMPA	16.0751	18.8125	**20.4488**	21.4567	27.2478	31.8160	38.0477	**42.0791**	44.2614	45.9047
	FFA	16.0751	18.8129	20.4452	21.4559	26.2709	29.5272	34.9981	38.8658	41.2281	42.7745
	SCA	**16.0827**	18.8924	20.4463	21.5307	27.1930	31.1098	35.8470	39.0601	41.1149	42.5819
	FPA	16.0768	18.8461	20.4374	21.4167	26.3792	30.1531	35.1931	38.0125	39.9903	42.4332
	L-SHADE	16.0179	18.6636	19.8807	**21.5476**	25.4422	29.3645	34.5157	37.3993	39.6480	41.5033
	SSA	16.0751	18.8125	20.4440	21.4246	26.6092	29.5688	34.5122	38.8826	40.4920	43.6145
	EO	16.0751	18.8125	**20.4488**	21.3566	26.7137	30.6354	35.0350	37.0585	39.6525	41.4923
	CSA	16.0748	18.8629	20.3635	21.4873	26.7369	30.6653	35.2753	38.6441	40.5772	42.1391

Table 5 (continued)

ID	Algorithm	Threshold level (n)									
		2-n	3-n	4-n	5-n	10-n	20-n	40-n	60-n	80-n	100-n
Mandrill	IWOA	**16.0224**	18.6845	20.4448	**22.1853**	**26.3722**	32.3825	38.6526	**42.5150**	**44.7773**	**46.9402**
	IMPA	**16.0224**	18.6644	20.4448	**22.1853**	26.3530	**32.6721**	**39.2602**	42.3941	44.5893	46.1535
	FFA	**16.0224**	18.6593	20.4327	**22.1853**	26.3572	32.1962	38.0196	40.9025	42.0967	43.7755
	SCA	16.0217	18.6987	20.3928	22.0788	25.6647	30.5413	35.5081	38.6804	40.2669	42.4611
	FPA	16.0223	18.7418	20.3279	22.0176	25.8664	29.9430	34.5191	37.3315	39.8083	41.9171
	L-SHADE	15.9707	18.5610	19.8114	21.0192	24.6964	28.9577	34.2195	37.0521	40.1598	41.6228
	SSA	**16.0224**	18.6543	20.4310	22.1887	26.5805	31.9945	38.0775	40.5521	42.3196	43.7486
	EO	**16.0224**	18.6795	20.4439	22.1817	26.0229	31.9824	37.8365	41.1402	42.9315	44.8846
	CSA	16.0222	**18.7012**	20.3947	21.9913	26.0366	30.5380	35.5805	38.6316	40.9571	42.9933
Lena	IWOA	**14.5905**	17.2956	18.9878	19.9951	26.2791	32.7712	38.6962	**42.2773**	**44.6147**	**46.7193**
	IMPA	**14.5905**	17.2956	**19.0590**	19.9951	**26.5888**	**32.8846**	**38.8096**	42.2573	44.1450	46.0416
	FFA	**14.5905**	17.2956	18.9663	**20.0024**	27.0062	32.5039	37.7317	40.2838	41.9336	44.4400
	SCA	14.5806	**17.3046**	18.9222	19.8514	24.8959	30.2306	35.2764	38.0468	40.4707	41.7868
	FPA	14.5894	17.2792	18.9582	19.7769	24.4228	29.6579	35.0304	37.8850	39.9406	42.0798
	L-SHADE	14.5626	17.1384	18.5966	19.2063	23.8421	29.0641	33.7940	37.5096	39.6289	41.4567
	SSA	**14.5905**	17.2956	19.0217	19.9985	26.9547	32.8229	37.8615	40.1590	42.6289	43.8999
	EO	**14.5905**	17.2956	19.0163	19.9951	26.8761	32.5363	37.8972	40.8029	42.8185	44.4948
	CSA	**14.5905**	17.2796	18.9372	19.9300	25.0691	30.7963	35.7561	38.9216	41.2209	42.8667

Bold values indicate the best value

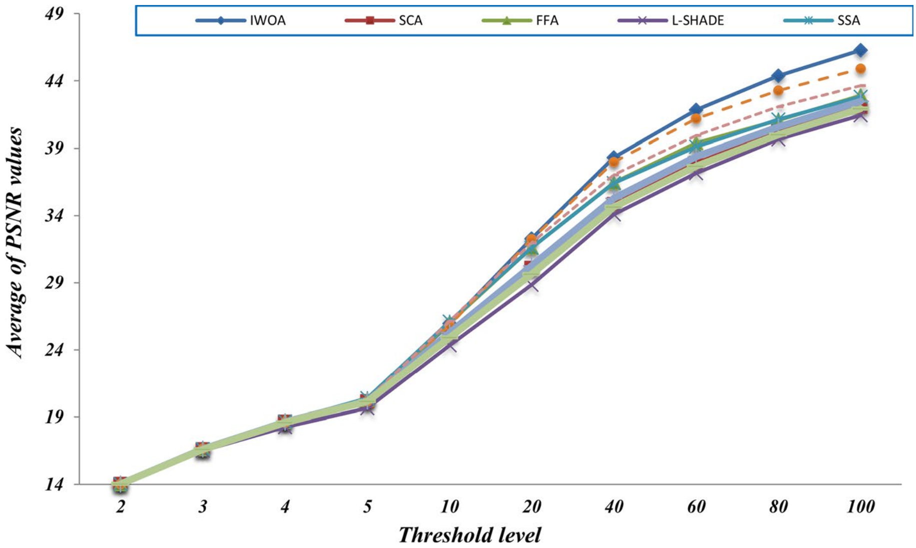

Fig. 13 Average PSNR values on each threshold level

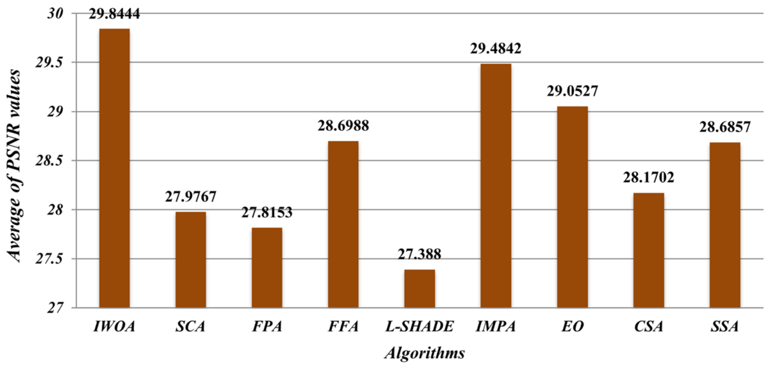

Fig. 14 PSNR values Comparison of the total average for all the test images

images. Figure 13 shows the total average PSNR values for each algorithm for each threshold level. The total average PSNR can be defined as:

$$Total_PSNR_{Avg} = \sum_{j=1}^{IN} PSNR_{Avg_j}, IN = 1, \ldots, 9 \tag{33}$$

where IN is the number of the used test images, which is 9. $PSNR_{Avg_j}$ is the j^{th} obtained average PSNR value for an image for a given threshold level. IWOA achieves the best results compared to the other algorithms, especially with the threshold level higher than 10. Also, Fig. 14 shows the summation of the total average PSNR values for all threshold

Table 6 The SSIM values obtained by each algorithm

ID	Algorithm	Threshold level (n)									
		2-n	3-n	4-n	5-n	10-n	20-n	40-n	60-n	80-n	100-n
61060	IWOA	0.8476	**0.8627**	**0.9413**	0.9499	**0.9839**	**0.9939**	**0.9968**	**0.9973**	**0.9976**	**0.9976**
	IMPA(Abdel-Basset et al. 2020)	0.8476	0.8574	0.9413	**0.953**	0.9839	0.993	0.9956	0.9964	0.9968	0.9972
	FFA (Erdmann et al. 2015)	0.8476	0.8521	0.9409	0.9497	0.9815	0.9905	0.9922	0.9942	0.9955	0.9958
	SCA (Mirjalili 2016)	**0.8476**	0.8511	0.9386	0.952	0.9805	0.9908	0.9953	0.9963	0.9969	0.9972
	FPA(Yang 2012)	0.8476	0.8497	0.9394	0.9508	0.9791	0.9888	0.9947	0.9961	0.9967	0.9971
	L-SHADE(Brest et al. 2016)	0.8357	0.8453	0.9205	0.94	0.9706	0.9876	0.9941	0.9952	0.9965	0.997
	SSA (Wang et al. 2020)	0.8476	0.856	0.9409	0.9508	0.9776	0.9894	0.9916	0.9948	0.9957	0.9962
	EO(Abdel-Basset et al. 2021)	0.8476	0.8600	0.9413	0.9499	0.9824	0.9913	0.9933	0.9948	0.9955	0.9963
	CSA(Moses et al. 2019)	0.8475	0.8510	0.9386	**0.9532**	0.9803	0.9905	0.9948	0.9958	0.9967	0.9971
105053	IWOA	0.0771	0.7117	**0.7268**	0.8263	0.95	0.9847	**0.9943**	**0.9956**	**0.9965**	**0.9969**
	IMPA(Abdel-Basset et al. 2020)	0.0771	0.7117	0.7179	0.8352	0.9461	**0.986**	**0.9943**	0.9956	0.9964	0.9967
	FFA (Erdmann et al. 2015)	0.0771	0.7119	0.724	**0.8449**	**0.954**	0.9842	0.992	0.9946	0.9953	0.9961
	SCA (Mirjalili 2016)	0.0739	0.7093	0.711	0.8442	0.9312	0.9665	0.9856	0.9919	0.9938	0.9947
	FPA(Yang 2012)	0.0764	0.7099	0.7113	0.8418	0.9272	0.9673	0.9868	0.992	0.9932	0.9952
	L-SHADE(Brest et al. 2016)	**0.1771**	0.643	0.6982	0.7632	0.8796	0.9548	0.9838	0.9903	0.993	0.9949
	SSA (Wang et al. 2020)	0.0771	**0.7124**	0.717	0.8322	0.9535	0.9834	0.9916	0.9942	0.9956	0.9962
	EO(Abdel-Basset et al. 2021)	0.1586	0.7117	0.7403	0.8577	0.9512	0.9858	0.9942	0.9955	0.9964	0.9966
	CSA(Moses et al. 2019)	0.0750	0.7097	0.7114	**0.8489**	0.9340	0.9719	0.9876	0.9928	0.9940	0.9956

Table 6 (continued)

ID	Algorithm	Threshold level (n)									
		2-n	3-n	4-n	5-n	10-n	20-n	40-n	60-n	80-n	100-n
181079	IWOA	0.5938	0.7673	**0.909**	0.929	**0.982**	**0.9928**	**0.9957**	**0.9963**	**0.9964**	**0.9966**
	IMPA(Abdel-Basset et al. 2020)	0.5938	0.7673	0.9088	0.929	**0.982**	0.9925	0.9955	0.996	0.9961	0.9963
	FFA (Erdmann et al. 2015)	0.5938	0.7673	0.9008	0.9296	0.9813	0.9907	0.9938	0.9945	0.9956	0.9958
	SCA (Mirjalili 2016)	0.5966	0.7683	0.9087	0.9278	0.977	0.989	0.9939	0.9953	0.996	0.9961
	FPA(Yang 2012)	0.5938	0.7655	0.9089	0.9294	0.9746	0.9884	0.9936	0.9951	0.996	0.9961
	L-SHADE(Brest et al. 2016)	**0.6263**	**0.8113**	0.8702	0.9124	0.9628	0.9868	0.9936	0.9949	0.9957	0.9961
	SSA (Wang et al. 2020)	0.5938	0.7672	0.9005	**0.93**	0.9812	0.9907	0.994	0.995	0.9954	0.9959
	EO(Abdel-Basset et al. 2021)	0.5938	0.7741	0.9105	0.9291	0.9816	0.9919	0.9947	0.9955	0.9958	0.9961
	CSA(Moses et al. 2019)	0.5947	0.7704	0.9093	0.9284	0.9777	0.9895	0.9942	0.9955	0.9958	0.9961
232038	IWOA	**0.6517**	0.7972	0.8863	0.9338	0.9735	**0.9941**	**0.9969**	**0.9973**	**0.9976**	**0.9977**
	IMPA(Abdel-Basset et al. 2020)	**0.6517**	0.7972	0.9065	0.932	0.9748	0.9934	0.9965	0.9972	0.9974	0.9976
	FFA (Erdmann et al. 2015)	**0.6517**	0.7972	0.9114	**0.9357**	**0.9779**	0.9923	0.9959	0.9969	0.9973	0.9975
	SCA (Mirjalili 2016)	0.6512	0.8004	0.9134	0.9309	0.9702	0.9895	0.9955	0.9964	0.997	0.9973
	FPA(Yang 2012)	0.6516	0.7982	**0.9238**	0.9278	0.9733	0.9902	0.9951	0.9966	0.997	0.9973
	L-SHADE(Brest et al. 2016)	0.6514	**0.8155**	0.8704	0.9047	0.9635	0.9843	0.9941	0.9962	0.9968	0.9972
	SSA (Wang et al. 2020)	**0.6517**	0.7972	0.911	0.9344	0.977	0.9929	0.9961	0.997	0.9973	0.9975
	EO(Abdel-Basset et al. 2021)	**0.6517**	0.7972	0.9187	0.9320	0.9782	0.9934	0.9966	0.9973	0.9975	0.9976
	CSA(Moses et al. 2019)	0.6516	0.7988	0.9235	0.9306	0.9720	0.9900	0.9955	0.9966	0.9971	0.9974

Table 6 (continued)

ID	Algorithm	Threshold level (n)									
		2-n	3-n	4-n	5-n	10-n	20-n	40-n	60-n	80-n	100-n
277095	IWOA	**0.7949**	0.8825	0.8953	0.9286	0.9709	**0.9833**	**0.9862**	**0.9868**	**0.9869**	**0.987**
	IMPA(Abdel-Basset et al. 2020)	**0.7949**	0.8766	0.8953	0.9304	0.9716	**0.9833**	0.986	0.9866	0.9868	0.9869
	FFA (Erdmann et al. 2015)	0.7941	**0.8845**	**0.9006**	0.9298	0.9717	0.9832	0.9858	0.9862	0.9865	0.9867
	SCA (Mirjalili 2016)	**0.7949**	0.8778	0.8958	0.9258	0.9647	0.979	0.9832	0.9854	0.9863	0.9866
	FPA(Yang 2012)	0.7952	0.8771	0.899	0.9261	0.9604	0.9761	0.9826	0.9852	0.9861	0.9864
	L-SHADE(Brest et al. 2016)	0.766	0.8328	0.8741	0.8923	0.9372	0.97	0.9811	0.9846	0.9854	0.9861
	SSA (Wang et al. 2020)	0.7941	0.8806	0.9008	**0.931**	**0.9721**	0.9831	0.9857	0.9861	0.9866	0.9868
	EO(Abdel-Basset et al. 2021)	**0.7949**	0.8835	0.8953	0.9277	0.9708	0.9829	0.9858	0.9865	0.9868	0.9869
	CSA(Moses et al. 2019)	0.7952	0.8820	0.8995	0.9261	0.9651	0.9769	0.9839	0.9854	0.9863	0.9865

Bold values indicate the best value

Table 7 The SSIM values obtained by each algorithm

ID	Algorithm	Threshold level (n)									
		2-n	3-n	4-n	5-n	10-n	20-n	40-n	60-n	80-n	100-n
299091	IWOA	**0.671**	**0.7613**	0.8346	0.8808	**0.9737**	**0.9932**	0.9966	**0.9972**	**0.9975**	**0.9976**
	IMPA(Abdel-Basset et al. 2020)	**0.671**	**0.7613**	0.8346	0.8619	0.9735	0.993	**0.9967**	**0.9972**	0.9974	0.9975
	FFA (Erdmann et al. 2015)	**0.671**	**0.7613**	0.8366	**0.911**	0.9736	0.992	0.9952	0.9964	0.9969	0.9971
	SCA (Mirjalili 2016)	0.6621	0.7554	**0.8374**	0.8854	0.9693	0.9855	0.9935	0.9956	0.9964	0.997
	FPA(Yang 2012)	0.67	0.7582	0.8367	0.8724	0.9703	0.9866	0.9936	0.9957	0.9964	0.9971
	L-SHADE(Brest et al. 2016)	0.664	0.7316	0.8143	0.8729	0.9527	0.9824	0.9925	0.9951	0.9962	0.9968
	SSA (Wang et al. 2020)	**0.671**	0.7612	0.8358	0.8779	0.9735	0.9916	0.9953	0.9962	0.997	0.9973
	EO(Abdel-Basset et al. 2021)	0.6710	0.7613	0.8346	0.8812	0.9783	0.9934	0.9960	0.9968	0.9972	0.9973
	CSA(Moses et al. 2019)	0.6700	0.7610	0.8337	0.8847	0.9704	0.9881	0.9945	0.9960	0.9968	0.9972
157055	IWOA	**0.8733**	0.919	0.9408	0.9479	**0.9825**	**0.9888**	**0.9909**	**0.9912**	**0.9914**	**0.9914**
	IMPA(Abdel-Basset et al. 2020)	**0.8733**	0.9191	0.9409	0.9479	0.9821	**0.9888**	0.9908	0.9911	0.9913	0.9913
	FFA (Erdmann et al. 2015)	**0.8733**	**0.9195**	**0.9411**	**0.9486**	0.9821	0.9877	0.9899	0.9906	0.9909	0.9911
	SCA (Mirjalili 2016)	0.8733	0.9184	0.9405	0.9457	0.9777	0.9861	0.9896	0.9905	0.9909	0.9911
	FPA(Yang 2012)	0.8732	0.9188	0.9359	0.9466	0.9767	0.9857	0.9895	0.9905	0.9909	0.9911
	L-SHADE(Brest et al. 2016)	0.8686	0.911	0.9268	0.9367	0.9686	0.9832	0.9889	0.9903	0.9908	0.9911
	SSA (Wang et al. 2020)	**0.8733**	0.9193	**0.9411**	0.9484	0.9817	0.9879	0.9901	0.9906	0.9909	0.9911
	EO(Abdel-Basset et al. 2021)	**0.8733**	0.9190	0.9409	0.9481	0.9822	0.9884	0.9902	0.9907	0.9910	0.9912
	CSA(Moses et al. 2019)	**0.8733**	0.9191	0.9394	0.9470	0.9787	0.9865	0.9898	0.9906	0.9909	0.9912

Table 7 (continued)

ID	Algorithm	Threshold level (n)									
		2-n	3-n	4-n	5-n	10-n	20-n	40-n	60-n	80-n	100-n
108070	IWOA	**0.3955**	0.5708	0.6933	0.7969	**0.9592**	0.9846	**0.9897**	**0.9904**	**0.9909**	**0.9911**
	IMPA(Abdel-Basset et al. 2020)	**0.3955**	0.5708	0.692	0.7712	0.9522	**0.9847**	0.9894	0.9901	0.9906	0.9909
	FFA (Erdmann et al. 2015)	**0.3955**	0.5708	**0.6998**	0.8001	0.965	0.9838	0.9881	0.9897	0.9904	0.9905
	SCA (Mirjalili 2016)	0.3954	**0.58**	0.685	0.8021	0.9488	0.9782	0.9859	0.9887	0.9897	0.9903
	FPA(Yang 2012)	**0.3955**	0.5764	0.6913	0.7953	0.9463	0.9774	0.9869	0.9888	0.9897	0.9905
	L-SHADE(Brest et al. 2016)	0.3855	0.5523	0.7178	0.7786	0.9297	0.9724	0.9852	0.9884	0.9895	0.9902
	SSA (Wang et al. 2020)	0.3955	0.5707	0.6975	**0.8179**	0.9546	0.9839	0.9887	0.9894	0.9903	0.9905
	EO(Abdel-Basset et al. 2021)	0.3955	0.5708	0.6920	0.8147	0.9692	0.9855	0.9895	0.9902	0.9908	0.9910
	CSA(Moses et al. 2019)	0.3955	0.5756	0.7023	0.7837	0.9487	0.9780	0.9870	0.9894	0.9900	0.9907
108082	IWOA	0.5318	0.6676	0.7614	0.8068	**0.935**	**0.9901**	**0.9954**	**0.9967**	**0.9971**	**0.9974**
	IMPA(Abdel-Basset et al. 2020)	0.5318	0.6703	0.7613	0.7947	0.9198	0.9886	0.995	0.9964	0.9968	0.9972
	FFA (Erdmann et al. 2015)	0.5318	0.6703	**0.7615**	**0.8144**	0.933	0.9883	0.9936	0.9957	0.9963	0.997
	SCA (Mirjalili 2016)	0.5318	0.6703	0.7612	0.8031	0.9296	0.9831	0.9929	0.9954	0.9965	0.9967
	FPA(Yang 2012)	0.5318	0.6701	0.7554	0.7999	0.9263	0.9844	0.9927	0.9956	0.9962	0.9969
	L-SHADE(Brest et al. 2016)	0.5313	0.6701	0.7386	0.8039	0.9248	0.9768	0.9917	0.995	0.9958	0.9966
	SSA (Wang et al. 2020)	0.5318	0.6693	0.7616	0.8152	0.9289	0.9887	0.9942	0.9959	0.9964	0.9969
	EO(Abdel-Basset et al. 2021)	0.5318	0.6703	0.7616	0.8122	0.9429	0.9889	0.9948	0.9963	0.9968	0.9971
	CSA(Moses et al. 2019)	**0.5319**	**0.6714**	0.7611	0.8049	0.9218	0.9846	0.9936	0.9956	0.9965	0.9970

Bold values indicate the best value

Table 8 The SSIM values obtained by each algorithm

ID	Algorithm	Threshold level (n)									
		2-n	3-n	4-n	5-n	10-n	20-n	40-n	60-n	80-n	100-n
Barbara	IWOA	**0.8834**	**0.9356**	**0.9574**	**0.9710**	0.9879	**0.9954**	**0.9974**	**0.9977**	**0.9979**	**0.9979**
	IMPA	**0.8834**	**0.9356**	**0.9574**	**0.9710**	0.9879	0.9951	0.9973	**0.9977**	0.9978	**0.9979**
	FFA	**0.8834**	**0.9356**	**0.9574**	**0.9710**	0.9876	0.9952	0.9971	0.9975	0.9977	0.9978
	SCA	0.8836	**0.9356**	**0.9574**	0.9707	0.9865	0.9930	0.9962	0.9973	0.9975	0.9977
	FPA	**0.8834**	**0.9356**	0.9560	0.9700	0.9854	0.9931	0.9964	0.9972	0.9975	0.9977
	L-SHADE	0.8813	0.9320	0.9533	0.9668	0.9838	0.9926	0.9961	0.9971	0.9975	0.9976
	SSA	**0.8834**	**0.9356**	0.9573	0.9710	0.9876	0.9951	0.9970	0.9975	0.9977	0.9978
	EO	**0.8834**	**0.9356**	**0.9574**	0.9710	**0.9880**	0.9951	0.9970	0.9975	0.9977	0.9978
	CSA	**0.8834**	**0.9356**	0.9573	0.9703	0.9862	0.9933	0.9966	0.9973	0.9976	0.9977
Airplane	IWOA	**0.9019**	0.9486	**0.9613**	0.9664	**0.9883**	**0.9948**	**0.9970**	**0.9975**	**0.9977**	**0.9978**
	IMPA	**0.9019**	0.9486	**0.9613**	0.9668	0.9881	0.9943	0.9969	**0.9975**	**0.9977**	**0.9978**
	FFA	**0.9019**	0.9486	**0.9613**	0.9668	0.9854	0.9900	0.9951	0.9967	0.9972	0.9974
	SCA	0.9013	**0.9488**	0.9610	**0.9673**	0.9871	0.9927	0.9958	0.9968	0.9973	0.9974
	FPA	0.9018	0.9486	0.9605	0.9665	0.9843	0.9907	0.9953	0.9966	0.9969	0.9974
	L-SHADE	0.8995	0.9455	0.9541	0.9630	0.9794	0.9891	0.9952	0.9963	0.9969	0.9972
	SSA	**0.9019**	0.9486	0.9612	0.9666	0.9866	0.9899	0.9947	0.9967	0.9971	0.9976
	EO	**0.9019**	0.9486	**0.9613**	0.9665	0.9870	0.9930	0.9956	0.9962	0.9969	0.9973
	CSA	0.9018	0.9487	0.9604	0.9671	0.9861	0.9918	0.9953	0.9967	0.9971	0.9973

Table 8 (continued)

ID	Algorithm	Threshold level (n)									
		2-n	3-n	4-n	5-n	10-n	20-n	40-n	60-n	80-n	100-n
Mandrill	IWOA	**0.8637**	0.9184	**0.9405**	0.9613	0.9835	0.9941	**0.9971**	**0.9975**	**0.9977**	**0.9978**
	IMPA	**0.8637**	0.9183	**0.9405**	0.9613	0.9835	**0.9944**	**0.9971**	**0.9975**	**0.9977**	0.9977
	FFA	**0.8637**	0.9182	**0.9405**	**0.9614**	0.9829	0.9936	0.9966	0.9972	0.9973	0.9975
	SCA	0.8636	0.9187	0.9400	0.9598	0.9792	0.9908	0.9954	0.9967	0.9969	0.9974
	FPA	**0.8637**	**0.9191**	0.9389	0.9586	0.9794	0.9894	0.9945	0.9960	0.9968	0.9973
	L-SHADE	0.8602	0.9131	0.9295	0.9439	0.9717	0.9859	0.9942	0.9959	0.9970	0.9972
	SSA	**0.8637**	0.9182	**0.9405**	**0.9614**	**0.9838**	0.9932	0.9967	0.9971	0.9974	0.9975
	EO	**0.8637**	0.9184	**0.9405**	0.9613	0.9819	0.9936	0.9966	0.9972	0.9975	0.9977
	CSA	**0.8637**	0.9185	0.9398	0.9588	0.9806	0.9907	0.9953	0.9966	0.9971	0.9975
Lena	IWOA	0.8295	0.9017	0.9296	**0.9400**	0.9823	**0.9949**	**0.9969**	**0.9975**	**0.9976**	**0.9978**
	IMPA	0.8295	0.9017	**0.9307**	**0.9400**	0.9842	**0.9949**	**0.9969**	**0.9975**	**0.9976**	**0.9978**
	FFA	0.8295	0.9017	0.9292	**0.9400**	0.9858	0.9943	0.9966	0.9971	0.9973	0.9977
	SCA	**0.8298**	**0.9025**	0.9284	0.9384	0.9745	0.9906	0.9954	0.9965	0.9972	0.9973
	FPA	0.8295	0.9016	0.9289	0.9371	0.9706	0.9896	0.9954	0.9965	0.9971	0.9973
	L-SHADE	0.8294	0.8978	0.9214	0.9279	0.9675	0.9885	0.9945	0.9963	0.9970	0.9972
	SSA	0.8295	0.9017	0.9301	**0.9400**	0.9854	0.9947	0.9966	0.9971	0.9973	0.9976
	EO	0.8295	0.9017	0.9300	**0.9400**	**0.9857**	0.9945	0.9967	0.9973	0.9974	0.9977
	CSA	0.8295	0.9015	0.9283	0.9387	0.9750	0.9919	0.9958	0.9968	0.9972	0.9974

Bold values indicate the best value

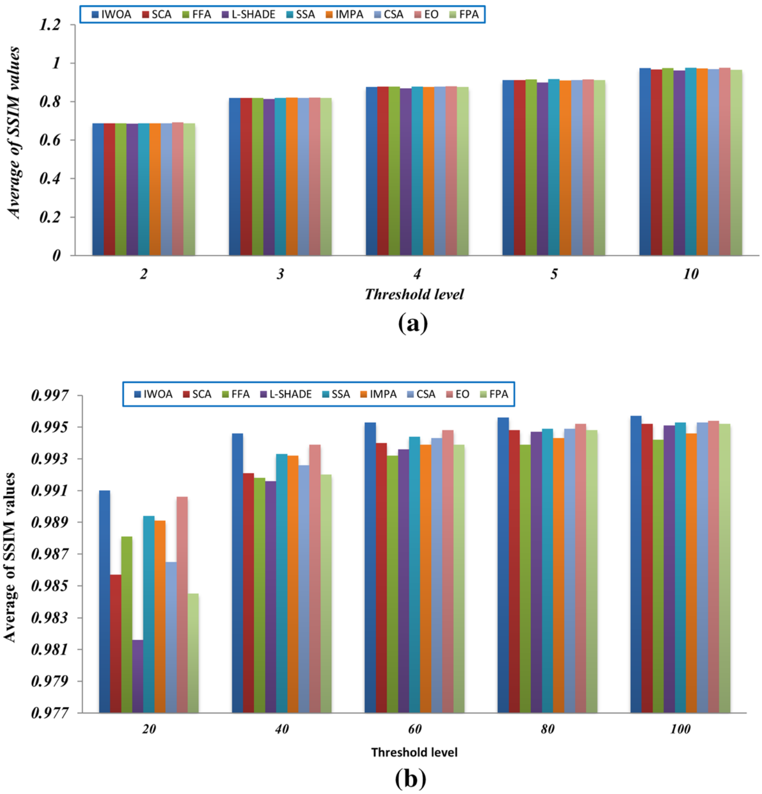

Fig. 15 Comparison among algorithms of the SSIM values

levels. The figure demonstrates the superiority of the proposed algorithm compared with the other algorithm in PSNR results. The higher PSNR values, the lower MSE values.

Tables 6, 7, and 8 provides the average SSIM values obtained by the algorithms on ten different threshold levels for all the test images. The SSIM metric is employed for assessing the structural similarity between the original image and the segmented image. According to the results, the proposed algorithm can also outperform the other algorithms for most of the test images on the different threshold values. Additionally, Fig. 15 inspects a comparison in terms of the total average SSIM for all the test images on each threshold level. The figure proves the efficacy of the proposed algorithm compared to the other algorithms with threshold levels higher than 10. With threshold levels smaller than 10, all algorithms seem to be converged.

Tables 9, 10, and 11 provides the average UQI values obtained by the algorithms on ten different threshold levels for all the test images. The UQI metric is also employed for assessing the structural similarity between the original image and the segmented image. According to the results, the proposed algorithm can also outperform the other algorithms for most of the test images on the different threshold values. Additionally, Fig. 16 inspects a comparison in terms of the total average SSIM for all the test images on each threshold level. The figure proves the efficacy of the proposed algorithm compared to the other

Table 9 The UQI values obtained by each algorithm

ID	Algorithm	Threshold level (n)									
		2-n	3-n	4-n	5-n	10-n	20-n	40-n	60-n	80-n	100-n
61060	IWOA	**0.8494**	**0.8722**	**0.9431**	0.9521	0.9861	**0.9960**	**0.9989**	**0.9994**	**0.9996**	**0.9997**
	IMPA	**0.8494**	0.8696	**0.9431**	**0.9549**	**0.9865**	0.9951	0.9981	0.9984	0.9991	0.9993
	FFA	**0.8494**	0.8537	0.9425	0.9540	0.9820	0.9918	0.9950	0.9967	0.9976	0.9983
	SCA	**0.8494**	0.8523	0.9411	0.9535	0.9836	0.9924	0.9971	0.9985	0.9991	0.9993
	FPA	**0.8494**	0.8523	0.9406	0.9526	0.9790	0.9919	0.9967	0.9984	0.9989	0.9993
	L-SHADE	0.8456	0.8465	0.9292	0.9402	0.9711	0.9893	0.9963	0.9980	0.9987	0.9992
	SSA	**0.8494**	0.8535	0.9428	0.9520	0.9796	0.9894	0.9940	0.9962	0.9976	0.9981
	EO	**0.8494**	**0.8722**	**0.9431**	0.9509	0.9832	0.9934	0.9952	0.9969	0.9976	0.9987
	CSA	**0.8494**	0.8526	0.9411	0.9544	0.9808	0.9922	0.9969	0.9982	0.9989	0.9991
61060	IWOA	0.0823	0.7153	0.7204	0.8283	0.9485	0.9867	**0.9965**	0.9979	**0.9987**	**0.9991**
	IMPA	0.0823	0.7153	0.7204	0.8549	0.9456	0.9880	**0.9965**	**0.9981**	**0.9987**	0.9987
	FFA	0.0823	0.7154	0.7202	0.8438	0.9513	0.9871	0.9955	0.9967	0.9977	0.9982
	SCA	0.0801	0.7115	0.7124	0.8440	0.9329	0.9673	0.9899	0.9940	0.9958	0.9975
	FPA	0.0821	0.7130	0.7145	0.8458	0.9248	0.9652	0.9877	0.9929	0.9964	0.9974
	L-SHADE	0.0803	0.6889	0.7314	0.7901	0.9152	0.9600	0.9864	0.9944	0.9961	0.9976
	SSA	0.0823	**0.7155**	0.7201	0.8543	**0.9547**	0.9871	0.9953	0.9964	0.9976	0.9982
	EO	**0.2041**	0.7153	**0.7429**	**0.8593**	0.9543	**0.9884**	0.9960	0.9979	0.9983	0.9988
	CSA	0.0813	0.7148	0.7144	0.8486	0.9467	0.9755	0.9912	0.9951	0.9972	0.9979

Table 9 (continued)

ID	Algorithm	Threshold level (n)									
		2-n	3-n	4-n	5-n	10-n	20-n	40-n	60-n	80-n	100-n
181079	IWOA	0.6007	0.7729	0.9136	**0.9338**	**0.9855**	**0.9962**	**0.9989**	**0.9995**	**0.9997**	**0.9998**
	IMPA	0.6007	0.7729	0.9132	**0.9338**	**0.9855**	0.9961	0.9986	0.9992	0.9994	0.9996
	FFA	0.6007	0.7729	0.9140	**0.9338**	0.9849	0.9941	0.9967	0.9981	0.9988	0.9992
	SCA	0.6020	0.7722	0.9128	0.9332	0.9806	0.9926	0.9971	0.9985	0.9992	0.9993
	FPA	0.6007	0.7720	0.9113	0.9318	0.9777	0.9919	0.9971	0.9984	0.9991	0.9994
	L-SHADE	**0.6141**	**0.7846**	0.9081	0.9226	0.9722	0.9894	0.9969	0.9983	0.9990	0.9994
	SSA	0.6007	0.7729	**0.9147**	**0.9338**	0.9848	0.9933	0.9968	0.9982	0.9986	0.9991
	EO	0.6007	0.7729	0.9137	0.9337	0.9851	0.9955	0.9979	0.9987	0.9989	0.9994
	CSA	0.6013	0.7738	0.9133	0.9324	0.9805	0.9930	0.9973	0.9987	0.9990	0.9994
232038	IWOA	0.6524	0.8012	0.9097	0.9233	0.9769	**0.9960**	**0.9988**	**0.9995**	**0.9997**	**0.9998**
	IMPA	0.6524	0.8012	0.9055	0.9335	0.9759	0.9953	0.9985	0.9993	0.9995	0.9997
	FFA	0.6524	0.8015	0.9104	0.9363	0.9798	0.9948	0.9981	0.9991	0.9995	0.9996
	SCA	0.6519	**0.8025**	0.9139	0.9279	0.9741	0.9931	0.9968	0.9988	0.9991	0.9994
	FPA	0.6524	0.8020	0.9242	0.9298	0.9721	0.9911	0.9972	0.9986	0.9991	0.9994
	L-SHADE	**0.6550**	0.7978	0.8787	0.9313	0.9704	0.9889	0.9965	0.9980	0.9990	0.9994
	SSA	0.6524	0.8019	0.9190	**0.9375**	0.9784	0.9950	0.9980	0.9991	0.9994	0.9996
	EO	0.6524	0.8012	0.9055	0.9339	**0.9802**	0.9956	0.9987	0.9993	0.9996	0.9997
	CSA	0.6523	0.8018	**0.9261**	0.9325	0.9738	0.9923	0.9976	0.9988	0.9993	0.9995

Table 9 (continued)

ID	Algorithm	Threshold level (n)									
		2-n	3-n	4-n	5-n	10-n	20-n	40-n	60-n	80-n	100-n
277095	IWOA	0.8066	0.8883	0.9077	0.9422	0.9833	**0.9960**	**0.9988**	**0.9994**	**0.9997**	**0.9998**
	IMPA	0.8066	0.8944	0.9077	**0.9441**	0.9841	**0.9960**	0.9987	0.9993	0.9995	0.9996
	FFA	0.8066	0.8931	0.9118	0.9437	**0.9844**	0.9955	0.9984	0.9988	0.9992	0.9994
	SCA	0.8070	0.8888	0.9072	0.9387	0.9789	0.9911	0.9968	0.9982	0.9989	0.9993
	FPA	0.8072	0.8895	0.9104	0.9372	0.9743	0.9880	0.9955	0.9976	0.9986	0.9990
	L-SHADE	0.8042	0.8754	0.9004	0.9186	0.9560	0.9826	0.9941	0.9969	0.9983	0.9988
	SSA	0.8066	0.8958	**0.9133**	0.9423	0.9843	0.9956	0.9982	0.9988	0.9991	0.9995
	EO	0.8066	**0.8948**	0.9116	0.9411	0.9837	0.9955	0.9985	0.9992	0.9994	0.9996
	CSA	**0.8081**	0.8897	0.9120	0.9404	0.9770	0.9900	0.9961	0.9982	0.9988	0.9992

Bold values indicate the best value

Table 10 The UQI values obtained by each algorithm

ID	Algorithm	Threshold level (n)									
		2-n	3-n	4-n	5-n	10-n	20-n	40-n	60-n	80-n	100-n
299091	IWOA	0.6720	**0.7634**	0.8357	0.8863	0.9761	0.9949	**0.9987**	**0.9993**	**0.9996**	**0.9997**
	IMPA	0.6720	**0.7634**	0.8357	0.8706	0.9750	0.9947	**0.9987**	**0.9993**	0.9995	0.9996
	FFA	0.6720	**0.7634**	0.8376	0.8931	0.9794	0.9942	0.9976	0.9986	0.9991	0.9994
	SCA	0.6669	0.7622	**0.8441**	0.8797	0.9652	0.9861	0.9953	0.9978	0.9987	0.9992
	FPA	0.6716	0.7622	0.8376	0.8754	0.9656	0.9880	0.9958	0.9979	0.9987	0.9992
	L-SHADE	**0.6722**	0.7293	0.8215	0.8779	0.9561	0.9829	0.9947	0.9975	0.9985	0.9989
	SSA	0.6720	**0.7634**	0.8363	**0.9089**	**0.9793**	0.9943	0.9974	0.9984	0.9991	0.9992
	EO	0.6720	**0.7634**	0.8357	0.9021	0.9802	**0.9955**	0.9983	0.9989	0.9993	0.9995
	CSA	0.6704	0.7611	0.8383	0.8880	0.9733	0.9899	0.9965	0.9984	0.9989	0.9992
157055	IWOA	**0.8813**	0.9272	0.9485	0.9564	**0.9908**	**0.9972**	**0.9992**	**0.9996**	**0.9998**	**0.9998**
	IMPA	**0.8813**	**0.9275**	0.9487	0.9563	0.9907	**0.9972**	**0.9992**	**0.9996**	0.9997	0.9998
	FFA	**0.8813**	**0.9275**	0.9487	**0.9567**	0.9903	0.9964	0.9983	0.9990	0.9993	0.9995
	SCA	0.8808	0.9271	**0.9488**	0.9549	0.9865	0.9945	0.9977	0.9990	0.9994	0.9996
	FPA	**0.8813**	0.9262	0.9448	0.9539	0.9843	0.9942	0.9980	0.9988	0.9993	0.9995
	L-SHADE	0.8797	0.9235	0.9403	0.9502	0.9804	0.9926	0.9976	0.9988	0.9992	0.9995
	SSA	**0.8813**	**0.9275**	0.9480	**0.9567**	0.9897	0.9964	0.9983	0.9990	0.9994	0.9995
	EO	**0.8813**	0.9274	0.9486	0.9564	0.9903	0.9966	0.9986	0.9991	0.9994	0.9996
	CSA	0.8812	0.9268	0.9475	0.9548	0.9868	0.9948	0.9981	0.9989	0.9994	0.9996

Table 10 (continued)

ID	Algorithm	Threshold level (n)									
		2-n	3-n	4-n	5-n	10-n	20-n	40-n	60-n	80-n	100-n
108070	IWOA	**0.4139**	0.5808	0.7064	0.8151	0.9666	0.9923	**0.9979**	**0.9989**	**0.9993**	**0.9995**
	IMPA	**0.4139**	0.5808	0.7064	0.7739	0.9627	0.9933	0.9975	0.9985	0.9991	0.9993
	FFA	**0.4139**	0.5808	**0.7093**	0.8241	0.9724	0.9930	0.9970	0.9982	0.9987	0.9991
	SCA	0.4130	**0.5897**	0.7078	0.8157	0.9592	0.9848	0.9939	0.9972	0.9982	0.9989
	FPA	**0.4139**	0.5836	0.6943	0.8219	0.9621	0.9855	0.9947	0.9971	0.9985	0.9989
	L-SHADE	0.4056	0.5866	0.6849	0.8005	0.9569	0.9781	0.9938	0.9973	0.9982	0.9987
	SSA	**0.4139**	0.5808	0.7065	**0.8249**	0.9726	0.9927	0.9968	0.9980	0.9987	0.9991
	EO	**0.4139**	0.5808	0.7064	0.8211	**0.9758**	**0.9942**	**0.9979**	0.9988	0.9992	0.9994
	CSA	**0.4139**	0.5872	0.6996	0.7916	0.9600	0.9876	0.9956	0.9976	0.9985	0.9990
108082	IWOA	0.5366	0.6803	0.7643	0.8129	0.9345	**0.9929**	**0.9980**	**0.9989**	**0.9994**	**0.9996**
	IMPA	0.5366	0.6839	0.7628	0.8043	0.9295	0.9915	0.9967	0.9984	0.9991	0.9994
	FFA	0.5369	0.6836	0.7665	0.8181	0.9458	0.9901	0.9960	0.9982	0.9989	0.9992
	SCA	0.5419	0.6799	0.7665	0.8091	0.9286	0.9858	0.9957	0.9974	0.9987	0.9990
	FPA	0.5368	0.6793	0.7697	**0.8191**	0.9284	0.9836	0.9956	0.9981	0.9986	0.9991
	L-SHADE	**0.5451**	0.6711	**0.7714**	0.8105	0.9252	0.9837	0.9953	0.9973	0.9987	0.9989
	SSA	0.5376	**0.6852**	0.7665	0.8165	0.9470	0.9893	0.9972	0.9983	0.9988	0.9992
	EO	0.5366	0.6839	0.7655	0.8149	**0.9554**	0.9896	0.9972	0.9984	0.9991	0.9994
	CSA	0.5382	0.6772	0.7658	**0.8124**	0.9315	0.9885	0.9963	0.9980	0.9985	0.9991

Bold values indicate the best value

Table 11 The UQI values obtained by each algorithm

ID	Algorithm	Threshold level (n)									
		2-n	3-n	4-n	5-n	10-n	20-n	40-n	60-n	80-n	100-n
Barbara	IWOA	0.8840	0.9366	**0.9585**	**0.9728**	**0.9899**	**0.9974**	**0.9993**	**0.9997**	**0.9998**	**0.9999**
	IMPA	0.8840	0.9366	**0.9585**	0.9727	0.9898	0.9971	**0.9993**	**0.9997**	0.9997	0.9998
	FFA	0.8840	0.9366	0.9584	0.9726	0.9895	0.9970	0.9991	0.9995	0.9996	0.9998
	SCA	**0.8841**	**0.9367**	**0.9585**	0.9724	0.9884	0.9952	0.9985	0.9992	0.9995	0.9997
	FPA	**0.8841**	0.9366	0.9579	0.9720	0.9874	0.9951	0.9984	0.9991	0.9995	0.9997
	L-SHADE	0.8838	0.9348	0.9558	0.9687	0.9862	0.9947	0.9981	0.9990	0.9994	0.9996
	SSA	0.8840	0.9366	0.9584	0.9726	0.9895	0.9970	0.9989	0.9994	0.9997	0.9997
	EO	0.8840	0.9366	**0.9585**	0.9727	0.9900	0.9971	0.9990	0.9994	0.9996	0.9997
	CSA	**0.8841**	0.9366	0.9580	0.9721	0.9883	0.9958	0.9985	0.9993	0.9996	0.9997
Airplane	IWOA	**0.9039**	**0.9510**	**0.9634**	0.9689	**0.9905**	**0.9968**	**0.9991**	**0.9995**	**0.9997**	**0.9998**
	IMPA	**0.9039**	**0.9510**	**0.9634**	**0.9694**	0.9902	0.9963	0.9989	**0.9995**	**0.9997**	0.9997
	FFA	**0.9039**	**0.9510**	0.9633	0.9689	0.9872	0.9925	0.9969	0.9986	0.9994	0.9994
	SCA	0.9035	0.9509	0.9635	0.9697	0.9892	0.9951	0.9977	0.9988	0.9992	0.9993
	FPA	**0.9039**	0.9509	0.9627	0.9687	0.9864	0.9928	0.9973	0.9986	0.9990	0.9994
	L-SHADE	0.9033	0.9467	0.9553	0.9632	0.9805	0.9926	0.9968	0.9983	0.9985	0.9993
	SSA	**0.9039**	**0.9510**	0.9633	0.9692	0.9887	0.9919	0.9968	0.9987	0.9991	0.9996
	EO	**0.9039**	**0.9510**	**0.9634**	0.9689	0.9892	0.9951	0.9973	0.9984	0.9990	0.9994
	CSA	0.9038	**0.9510**	**0.9634**	0.9688	0.9881	0.9946	0.9977	0.9989	0.9992	0.9995

Table 11 (continued)

ID	Algorithm	Threshold level (n)									
		2-n	3-n	4-n	5-n	10-n	20-n	40-n	60-n	80-n	100-n
Mandrill	IWOA	**0.8643**	0.9202	**0.9426**	0.9630	0.9855	0.9960	0.9989	**0.9995**	**0.9997**	**0.9998**
	IMPA	**0.8643**	0.9199	**0.9426**	0.9630	0.9854	**0.9964**	**0.9991**	0.9994	0.9996	0.9997
	FFA	**0.8643**	0.9202	0.9424	0.9632	0.9850	0.9959	0.9986	0.9991	0.9994	0.9996
	SCA	**0.8643**	0.9204	0.9417	0.9622	0.9816	0.9924	0.9970	0.9984	0.9990	0.9993
	FPA	**0.8643**	0.9210	0.9407	0.9604	0.9813	0.9914	0.9965	0.9980	0.9988	0.9992
	L-SHADE	0.8617	0.9118	0.9287	0.9414	0.9736	0.9869	0.9960	0.9981	0.9988	0.9992
	SSA	**0.8643**	0.9198	0.9425	**0.9631**	**0.9857**	0.9952	0.9986	0.9991	0.9994	0.9995
	EO	**0.8643**	0.9202	0.9425	0.9630	0.9835	0.9956	0.9987	0.9991	0.9995	0.9996
	CSA	**0.8643**	**0.9208**	0.9415	0.9611	0.9810	0.9927	0.9974	0.9986	0.9992	0.9994
Lena	IWOA	**0.8330**	0.9045	0.9319	0.9424	0.9845	**0.9970**	**0.9991**	**0.9996**	**0.9997**	**0.9998**
	IMPA	**0.8330**	0.9045	**0.9328**	0.9424	0.9864	**0.9970**	**0.9991**	0.9995	**0.9997**	**0.9998**
	FFA	**0.8330**	**0.9046**	0.9322	**0.9425**	**0.9879**	0.9967	0.9986	0.9993	0.9995	0.9996
	SCA	0.8329	0.9045	0.9326	0.9412	0.9749	0.9933	0.9978	0.9987	0.9990	0.9994
	FPA	**0.8330**	0.9043	0.9317	0.9396	0.9730	0.9918	0.9975	0.9986	0.9991	0.9994
	L-SHADE	0.8307	0.9000	0.9241	0.9351	0.9707	0.9906	0.9969	0.9983	0.9991	0.9994
	SSA	**0.8330**	0.9045	0.9324	**0.9425**	0.9877	0.9967	0.9987	0.9992	0.9995	0.9996
	EO	**0.8330**	0.9045	0.9313	0.9424	**0.9879**	0.9966	0.9988	0.9993	0.9995	0.9997
	CSA	**0.8330**	0.9040	0.9318	0.9413	0.9785	0.9936	0.9979	0.9989	0.9993	0.9995

Bold values indicate the best value

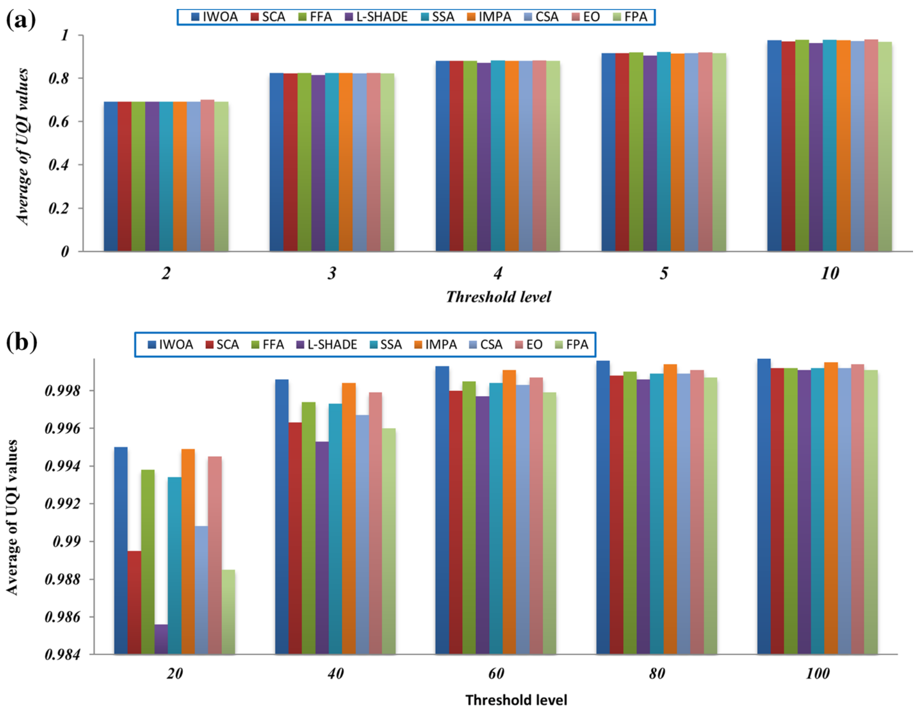

Fig. 16 Comparison among algorithms of the UQI values

algorithms with threshold levels higher than 10. With threshold levels smaller than 10, all algorithms seem to be converged.

Here, we are interested in comparing the algorithms in terms of maximizing Kapur's entropy function (Eq. 4). Regarding the results, we can observe that the proposed algorithm could be superior in most cases, especially cases with the high threshold levels, shown in Tables 12, 13, 14 and competitive in the other cases. Additionally, Fig. 17 illustrates the superiority of the proposed algorithm compared with the other algorithm in the Fitness values. The figure inspects the average fitness values for all the test images for each algorithm. IWOA achieves the highest fitness value of 53.7909, while IMPA comes in the second rank with 53.099. L-SHADE shows the lowest fitness value of 49.13.

Figure 18 demonstrates the average of the STD for the fitness values by running each algorithm 30 times on all test images for all threshold levels. Based on those results, the proposed algorithm could also outperform all the algorithms with an average value for STD of 0.2493. Figure 19 shows a comparison among the algorithms in terms of the CPU time. The figure provides the total CPU time for running each algorithm 30 using different threshold values for all the test images. Although IWOA doesn't obtain the minimum CPU time, it can achieve the best results for PSNR, SSIM, fitness, and STD. IWOA takes CPU time of 0.5385 seconds, while IMPA takes the most CPU time with a value of 0.9808. FFA succeeds to attain less time in 0.3318 seconds. We can conclude that IWOA attains the best results with less STD at a reasonable time when compared with other algorithms.

Table 12 The Fitness values obtained by each algorithm

ID	Algorithm	Threshold level (n)									
		2-n	3-n	4-n	5-n	10-n	20-n	40-n	60-n	80-n	100-n
61060	IWOA	**12.776**	15.9511	**19.0715**	21.789	33.8015	**52.3957**	**78.3952**	**96.322**	**109.6184**	**120.0533**
	IMPA(Abdel-Basset et al. 2020)	**12.776**	15.9561	**19.0715**	**21.8197**	**33.8031**	52.2547	77.7866	95.1371	107.3739	116.0695
	FFA (Erdmann et al. 2015)	**12.776**	**15.9611**	19.0712	21.788	33.7471	51.8177	75.8089	91.5198	103.0224	111.9054
	SCA (Mirjalili 2016)	12.7756	15.957	19.0357	21.7388	33.45	50.6662	73.1764	88.8787	100.2654	109.332
	FPA(Yang 2012)	**12.776**	15.9529	19.0336	21.7037	33.3017	50.2076	72.8298	88.225	100.0461	109.6068
	L-SHADE(Brest et al. 2016)	12.7402	15.848	18.7631	21.3867	32.6433	49.0551	70.8876	86.3258	98.1304	107.4438
	SSA (Wang et al. 2020)	**12.776**	15.9574	19.0712	21.7995	33.6629	51.7207	76.1782	91.5312	103.1833	112.8129
	EO(Abdel-Basset et al. 2021)	**12.7760**	15.9536	**19.0715**	21.7891	33.7511	51.7728	76.2052	92.0687	103.9213	113.4531
	CSA(Moses et al. 2019)	12.7759	15.9574	19.0516	21.7625	33.4716	50.8725	73.7686	89.3058	101.4225	110.6946
105053	IWOA	**11.8823**	**15.122**	18.0216	20.6712	**32.3523**	**50.3743**	**74.7683**	**91.2218**	**102.9993**	**112.056**
	IMPA(Abdel-Basset et al. 2020)	**11.8823**	**15.122**	**18.0383**	**20.6791**	32.3437	50.2377	74.2076	89.9192	100.9974	108.9814
	FFA (Erdmann et al. 2015)	**11.8823**	**15.122**	18.0247	**20.6791**	32.1936	49.4224	71.4182	85.7842	95.8659	104.189
	SCA (Mirjalili 2016)	11.881	15.113	17.9904	20.6263	31.9543	48.4581	69.2537	83.0938	93.5198	101.607
	FPA(Yang 2012)	11.8822	15.1112	17.9834	20.6066	31.7961	47.7961	68.4096	82.1473	92.5227	100.9397
	L-SHADE(Brest et al. 2016)	11.7392	14.8633	17.589	20.1722	30.8293	45.98	66.0778	79.8543	90.5128	98.9473
	SSA (Wang et al. 2020)	**11.8823**	15.1219	18.0358	20.6664	32.2229	49.4192	71.5406	85.3184	95.8636	104.4071
	EO(Abdel-Basset et al. 2021)	11.8482	**15.1220**	17.9966	**20.6998**	32.3109	49.7221	72.1895	86.1353	97.3854	104.7356
	CSA(Moses et al. 2019)	11.8821	15.1161	17.9991	20.6338	32.0011	48.5745	69.8052	84.2199	94.7203	103.0389

Table 12 (continued)

ID	Algorithm	Threshold level (n)									
		2-n	3-n	4-n	5-n	10-n	20-n	40-n	60-n	80-n	100-n
181079	IWOA	**12.5194**	**15.6559**	18.5605	21.2831	**33.0229**	**51.7113**	**77.6138**	**95.1912**	**108.2282**	**118.3517**
	IMPA(Abdel-Basset et al. 2020)	**12.5194**	**15.6559**	**18.5607**	**21.2833**	33.0227	51.5554	77.0396	93.8592	105.3401	114.4753
	FFA (Erdmann et al. 2015)	**12.5194**	**15.6559**	18.5596	21.2816	32.9363	51.0539	74.4852	89.7446	101.5361	110.4897
	SCA (Mirjalili 2016)	12.5193	15.6528	18.5481	21.2574	32.7656	50.0573	72.2192	87.5166	98.8036	107.7341
	FPA(Yang 2012)	**12.5194**	15.6525	18.5463	21.2322	32.5791	49.4161	71.6639	86.8136	98.6199	107.5495
	L-SHADE(Brest et al. 2016)	12.5021	15.5605	18.3787	20.9216	31.8685	48.2518	69.8864	84.675	96.4386	105.7433
	SSA (Wang et al. 2020)	**12.5194**	15.6559	18.56	21.2813	32.9585	51.1506	74.8946	90.6978	101.2136	110.3164
	EO(Abdel-Basset et al. 2021)	**12.5194**	15.6530	18.5598	21.2829	32.9412	51.0342	74.8979	90.8307	102.4668	111.2834
	CSA(Moses et al. 2019)	12.5194	15.6545	18.5530	21.2561	32.7245	49.9210	72.6653	88.2450	99.7304	109.0304
232038	IWOA	**11.9894**	**15.2615**	18.0564	20.8226	32.5819	**50.9049**	**76.2528**	**93.5106**	**106.3026**	**116.2968**
	IMPA(Abdel-Basset et al. 2020)	**11.9894**	**15.2615**	**18.0657**	**20.8512**	**32.5896**	50.6511	75.6467	92.4374	104.1028	112.7034
	FFA (Erdmann et al. 2015)	**11.9894**	15.2606	18.0551	20.7902	32.4147	50.1182	73.7958	89.8715	100.9383	109.7447
	SCA (Mirjalili 2016)	11.9891	15.249	18.022	20.7231	32.1319	49.1496	71.225	85.6759	96.8546	105.4877
	FPA(Yang 2012)	11.9893	15.2502	18.025	20.7002	31.9145	48.6638	70.3656	85.5129	96.7159	105.5622
	L-SHADE(Brest et al. 2016)	11.9613	15.0528	17.7702	20.3541	31.1784	47.232	68.699	83.3479	94.5921	103.6789
	SSA (Wang et al. 2020)	**11.9894**	15.261	18.0619	20.8162	32.4102	50.1126	74.0407	90.1449	101.0976	110.3437
	EO(Abdel-Basset et al. 2021)	**11.9894**	**15.2615**	**18.0687**	**20.8512**	32.5406	50.1159	74.1409	90.2424	101.5987	110.4611
	CSA(Moses et al. 2019)	11.9894	15.2547	18.0412	20.7296	32.2061	49.0106	71.4365	86.6975	98.2346	106.9818

Table 12 (continued)

ID	Algorithm	Threshold level (n)									
		2-n	3-n	4-n	5-n	10-n	20-n	40-n	60-n	80-n	100-n
277095	IWOA	**11.9706**	**14.9796**	**17.802**	20.4036	**31.6016**	**48.2872**	**70.2967**	**84.8372**	**95.0545**	**102.9802**
	IMPA(Abdel-Basset et al. 2020)	**11.9706**	14.9795	**17.802**	**20.4091**	31.5793	48.2265	69.9503	83.2584	91.978	98.399
	FFA (Erdmann et al. 2015)	**11.9706**	14.9793	17.7932	20.3993	31.5387	47.9795	68.6196	80.9031	89.0562	95.4017
	SCA (Mirjalili 2016)	11.9703	14.9777	17.7794	20.3582	31.2482	46.4847	65.0903	77.2917	86.0844	92.7041
	FPA(Yang 2012)	11.9706	14.9763	17.7676	20.3349	30.9178	45.3584	62.8773	74.6368	83.5616	90.2943
	L-SHADE(Brest et al. 2016)	11.9036	14.8163	17.5314	19.8222	29.1678	42.401	59.4692	71.5032	79.9929	86.9559
	SSA (Wang et al. 2020)	**11.9706**	14.9791	17.7927	20.4005	31.5368	47.8578	67.9296	80.6834	89.2749	96.6264
	EO(Abdel-Basset et al. 2021)	**11.9706**	**14.9797**	**17.8020**	20.4010	31.5495	47.7624	68.4138	81.7316	90.9752	98.3387
	CSA(Moses et al. 2019)	11.9704	14.9777	17.7781	20.3590	31.1246	46.0247	64.5108	76.7458	85.4095	92.4490

Bold values indicate the best value

Table 13 The Fitness values obtained by each algorithm

ID	Algorithm	Threshold level (n)									
		2-n	3-n	4-n	5-n	10-n	20-n	40-n	60-n	80-n	100-n
299091	IWOA	**12.1936**	**15.2182**	**18.06**	**20.6625**	**32.037**	**48.9849**	**72.2013**	**87.63**	**98.821**	**107.3364**
	IMPA(Abdel-Basset et al. 2020)	**12.1936**	**15.2182**	**18.06**	20.6617	32.0308	48.8686	71.6678	86.1093	96.4726	103.7719
	FFA (Erdmann et al. 2015)	**12.1936**	**15.2182**	18.0594	20.6612	31.8862	47.9939	68.2067	81.2467	90.8543	98.5
	SCA (Mirjalili 2016)	12.1935	15.2127	18.0461	20.6218	31.6553	46.9312	66.3038	79.1904	88.7332	96.069
	FPA(Yang 2012)	**12.1936**	15.2134	18.0392	20.6098	31.3523	46.2153	65.2326	78.1287	87.5557	95.305
	L-SHADE(Brest et al. 2016)	12.1758	15.1165	17.7635	20.2311	29.9142	43.4662	61.9724	75.148	84.9238	92.8362
	SSA (Wang et al. 2020)	**12.1936**	15.218	18.0595	20.6608	31.8082	47.9178	68.1283	81.1228	91.3473	98.9493
	EO(Abdel-Basset et al. 2021)	**12.1936**	**15.2182**	**18.0600**	20.6615	31.9104	48.1877	68.5090	81.7795	91.5729	99.0036
	CSA(Moses et al. 2019)	12.1936	15.2150	18.0423	20.6216	31.6156	47.0079	66.6733	79.8625	89.8023	97.4248
157055	IWOA	**12.7329**	**15.8481**	**18.7846**	**21.5883**	**33.58**	**51.5129**	**76.3282**	**93.3345**	**105.7084**	**115.3345**
	IMPA(Abdel-Basset et al. 2020)	**12.7329**	**15.8481**	**18.7846**	**21.5883**	33.5438	51.4185	75.8986	91.9737	103.1469	111.9807
	FFA (Erdmann et al. 2015)	**12.7329**	**15.8481**	18.7841	21.5846	33.5169	50.5955	73.2913	87.9072	99.147	107.5119
	SCA (Mirjalili 2016)	12.7324	15.8465	18.7767	21.5452	33.0927	49.846	71.1477	85.6086	96.1502	105.1024
	FPA(Yang 2012)	12.7327	15.8464	18.7693	21.5363	32.9778	49.1333	70.239	84.7424	95.9082	104.5418
	L-SHADE(Brest et al. 2016)	12.7131	15.7919	18.6232	21.2728	32.1838	47.8387	68.3398	82.6632	93.9342	102.6285
	SSA (Wang et al. 2020)	**12.7329**	15.8481	18.7843	21.5851	33.5003	50.5414	73.4454	87.7362	98.669	107.3931
	EO(Abdel-Basset et al. 2021)	**12.7329**	**15.8481**	18.7845	21.5880	33.5399	50.8141	73.7899	88.6606	99.8075	108.0157
	CSA(Moses et al. 2019)	12.7326	15.8470	18.7751	21.5526	33.1433	49.8022	71.5882	86.0455	97.1117	105.9712

Table 13 (continued)

ID	Algorithm	Threshold level (n)									
		2-n	3-n	4-n	5-n	10-n	20-n	40-n	60-n	80-n	100-n
108070	IWOA	**12.5289**	**15.7032**	18.5777	21.2449	**32.9399**	**50.7339**	**74.9149**	**91.1513**	**103.1007**	**112.4513**
	IMPA(Abdel-Basset et al. 2020)	**12.5289**	**15.7032**	**18.5786**	**21.2508**	32.9194	50.6107	74.2717	89.7181	100.1829	108.4918
	FFA (Erdmann et al. 2015)	**12.5289**	**15.7032**	18.5733	21.24	32.8684	50.017	72.3464	86.2931	96.7648	104.4112
	SCA (Mirjalili 2016)	12.5284	15.6982	18.5556	21.22	32.6078	48.9772	69.7404	83.4832	93.6996	101.6287
	FPA(Yang 2012)	**12.5289**	15.6973	18.5418	21.1986	32.4195	48.3326	69.3536	83.2895	93.5883	101.5344
	L-SHADE(Brest et al. 2016)	12.495	15.6113	18.4059	20.9844	31.7188	47.1881	67.1581	81.5701	91.8702	100.0146
	SSA (Wang et al. 2020)	**12.5289**	15.7031	18.575	21.2338	32.8494	50.0621	71.945	86.1112	96.6926	104.2336
	EO(Abdel-Basset et al. 2021)	**12.5289**	**15.7032**	**18.5786**	21.2380	32.8913	50.1531	72.7822	87.1156	97.9495	106.3171
	CSA(Moses et al. 2019)	12.5289	15.6980	18.5549	21.2202	32.6136	48.9436	70.3134	84.5232	95.2522	103.4803
108082	IWOA	**12.5693**	**15.8063**	18.8163	21.5944	33.5664	**52.3813**	**78.7126**	**96.9154**	**110.5434**	**121.0727**
	IMPA(Abdel-Basset et al. 2020)	**12.5693**	**15.8063**	**18.8167**	**21.5958**	**33.5708**	52.1202	77.9697	95.755	107.9924	117.6285
	FFA (Erdmann et al. 2015)	**12.5693**	**15.8063**	18.8159	21.5932	33.4895	51.6847	75.954	92.9873	104.651	114.27
	SCA (Mirjalili 2016)	**12.5693**	15.8046	18.8083	21.5741	33.2802	50.6619	73.6094	89.4522	101.3693	110.538
	FPA(Yang 2012)	**12.5693**	15.8043	18.8031	21.5577	33.1035	50.2587	73.2679	89.2795	101.1707	110.884
	L-SHADE(Brest et al. 2016)	12.5569	15.7491	18.6537	21.3417	32.5185	49.0634	71.6566	87.5361	99.5521	109.1102
	SSA (Wang et al. 2020)	**12.5693**	15.8062	18.8158	21.593	33.466	51.7307	76.3116	93.0452	104.5969	113.8966
	EO(Abdel-Basset et al. 2021)	**12.5693**	**15.8063**	18.8160	21.5936	33.4811	51.7049	76.5644	93.0660	105.0594	114.6498
	CSA(Moses et al. 2019)	**12.5693**	15.8049	18.8087	21.5746	33.2841	50.7958	74.0185	89.8674	102.3192	111.9132

Bold values indicate the best value

Table 14 The Fitness values obtained by each algorithm

ID	Algorithm	Threshold level (n)									
		2-n	3-n	4-n	5-n	10-n	20-n	40-n	60-n	80-n	100-n
Barbara	IWOA	**12.8944**	**16.0776**	**19.0524**	**21.8663**	**33.9123**	**52.4601**	**79.0757**	**97.5044**	**111.1390**	**121.6892**
	IMPA	**12.8944**	**16.0776**	**19.0524**	**21.8663**	33.8879	52.2651	78.4649	96.2442	108.8346	119.0990
	FFA	**12.8944**	16.0775	19.0523	21.8658	33.8054	51.8108	76.8774	93.3866	105.6021	114.8431
	SCA	**12.8944**	16.0758	19.0482	21.8492	33.6107	50.7942	73.8078	89.7958	101.6265	111.2091
	FPA	**12.8944**	16.0756	19.0413	21.8341	33.3758	50.3978	73.7337	89.6948	102.0421	111.8403
	L-SHADE	12.8922	16.0579	18.9910	21.7421	33.0279	49.9484	72.8420	88.7265	100.7691	110.3752
	SSA	**12.8944**	16.0775	19.0523	21.8659	33.7984	51.7781	76.6527	93.2786	105.3635	114.6159
	EO	**12.8944**	**16.0776**	**19.0524**	**21.8663**	33.8446	51.9086	76.6778	93.4764	106.5393	115.7284
	CSA	**12.8944**	16.0764	19.0476	21.8471	33.5953	50.8853	74.2599	90.3407	103.0055	112.4235
Airplane	IWOA	**12.2274**	**15.5081**	**18.3280**	20.9303	32.1921	**49.4457**	**73.3265**	**89.5468**	**101.3674**	**110.3298**
	IMPA	**12.2274**	**15.5081**	**18.3280**	**20.9443**	**32.1938**	49.3655	72.9529	88.3452	99.0658	107.5168
	FFA	**12.2274**	**15.5081**	18.3277	20.9426	32.1144	48.7340	71.0379	85.4506	95.3996	103.3912
	SCA	12.2271	15.5060	18.3131	20.9008	31.8910	47.6428	68.1025	81.4938	91.3694	99.3757
	FPA	**12.2274**	15.5050	18.3041	20.8828	31.5846	46.8968	66.7783	80.3438	90.4299	98.7316
	L-SHADE	12.2193	15.4624	18.1729	20.6912	31.0167	45.4572	65.3350	78.7339	89.0651	97.3590
	SSA	**12.2274**	**15.5081**	18.3276	20.9398	32.1214	48.8001	70.8753	85.1912	95.0733	103.6766
	EO	**12.2274**	**15.5081**	**18.3280**	20.9323	32.1053	48.7336	71.1307	85.3082	96.0334	104.1792
	CSA	12.2273	15.5069	18.3155	20.9039	31.8410	47.6095	68.4197	82.4731	93.1874	101.3812

Table 14 (continued)

ID	Algorithm	Threshold level (n)									
		2-n	3-n	4-n	5-n	10-n	20-n	40-n	60-n	80-n	100-n
Mandrill	IWOA	**12.2772**	**15.3757**	**18.2736**	**20.9959**	**32.9155**	51.1552	**76.0453**	**92.9924**	**105.3956**	**114.9888**
	IMPA	**12.2772**	**15.3757**	**18.2736**	**20.9959**	32.9143	51.1099	75.6127	91.7131	103.1385	112.2372
	FFA	**12.2772**	**15.3757**	**18.2736**	20.9950	32.7840	50.5569	73.9999	89.7650	100.2964	108.6361
	SCA	**12.2772**	15.3750	18.2694	20.9754	32.5856	49.3850	70.8031	85.1097	95.4408	103.8036
	FPA	**12.2772**	15.3742	18.2574	20.9455	32.3696	48.6056	69.7875	83.8852	94.5511	103.5075
	L-SHADE	12.2716	15.3496	18.1481	20.7558	31.8418	47.5229	68.1328	82.4165	93.4220	102.1532
	SSA	**12.2772**	**15.3757**	18.2735	20.9946	32.7925	50.3889	73.9087	89.0713	100.4362	108.8014
	EO	**12.2772**	**15.3757**	**18.2736**	20.9956	32.8209	50.6321	74.1493	89.5809	100.6387	109.2418
	CSA	**12.2772**	15.3748	18.2661	20.9636	32.5732	49.4223	71.0083	85.4344	96.6188	105.3668
Lena	IWOA	**12.4048**	**15.4167**	18.1576	**20.8085**	32.0524	**49.6385**	**74.1868**	**90.5829**	**102.7917**	**112.0831**
	IMPA	**12.4048**	**15.4167**	**18.1610**	**20.8085**	**32.0648**	**49.5704**	**73.5401**	**89.6584**	**100.5093**	**109.4049**
	FFA	**12.4048**	**15.4167**	18.1575	20.8062	31.9091	48.9252	71.3114	85.7903	95.9802	104.9155
	SCA	12.4044	15.4150	18.1452	20.7724	31.6910	47.8182	68.6007	82.6401	92.7791	100.4986
	FPA	**12.4048**	15.4150	18.1412	20.7472	31.4874	47.2013	67.6995	81.6370	92.0589	100.1660
	L-SHADE	12.3984	15.3854	18.0679	20.5629	31.0228	46.3283	66.1567	80.2060	90.6329	99.0467
	SSA	**12.4048**	**15.4167**	18.1581	20.8081	31.9273	48.7946	71.3387	85.9434	96.7511	104.2898
	EO	**12.4048**	**15.4167**	18.1593	**20.8085**	31.9498	49.0792	71.6291	86.3202	97.0603	105.3507
	CSA	**12.4048**	15.4154	18.1476	20.7676	31.6884	47.9890	69.2904	83.6876	94.4701	102.7164

Bold values indicate the best value

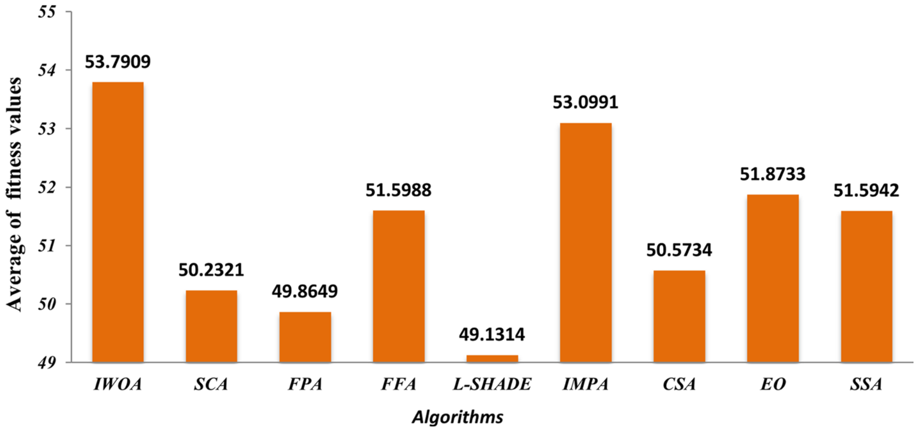

Fig. 17 Comparison of the Fitness values results from each algorithm

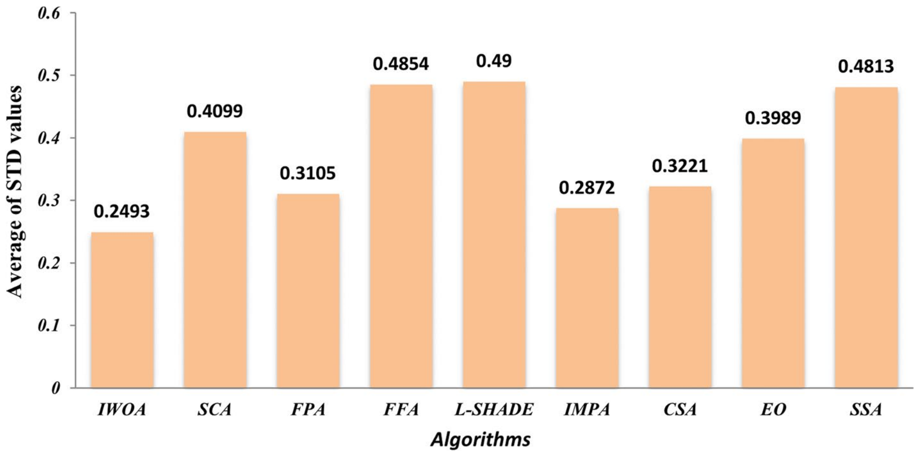

Fig. 18 Average STD for fitness values of all test images on all threshold levels

6.6 The segmented Images

Figure 20 presents the segmented images generated by the proposed algorithm using ten different threshold levels. We can see that using more threshold levels makes the segmented image to be better and close to the original one. For using a 100-threshold level, we can see that the segmented image is the best compared to other threshold levels as it succeeds to separate more objects.

6.7 Wilcoxon rank-sum test

In this section, the results obtained by our proposed algorithm are compared with the results obtained by the other algorithms using the statistical test called the Wilcoxon rank-sum test (Haynes 2013). This test is based on the null hypothesis and the alternative

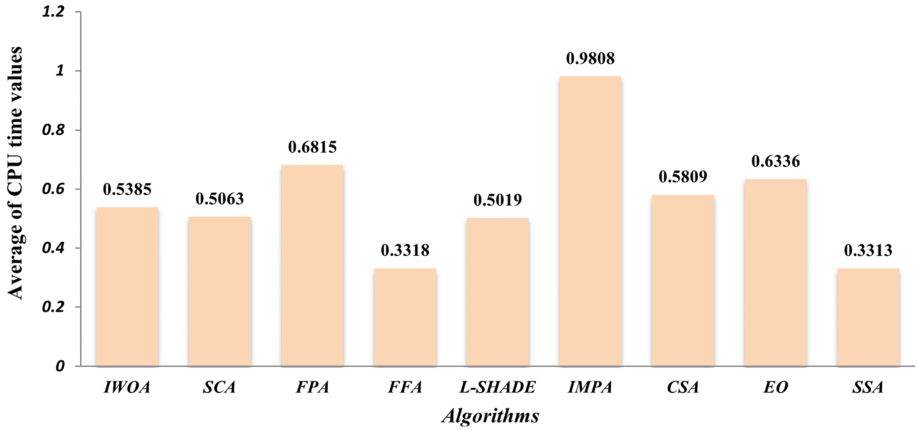

Fig. 19 Average CPU Time values for all test images on all threshold levels

Fig. 20 The segmented images were obtained by the proposed algorithm using threshold levels 2, 3,4,5,10, 20, 40, and 100, respectively

hypothesis. In the null hypothesis, this test supposes that there is no difference between the ranks of the results obtained by a pair of algorithms. On the other hand, the alternative hypothesis considers that there is a difference between the ranks obtained by a pair of algorithms. The significant level used in our test is 5%. Tables 15, 16, and 17 show the P and S values obtained by comparing the fitness values obtained by the proposed algorithm with those of each compared algorithm on nine test images: 61060, 105053, 181079, 232038, 277095, 299091, 157055, 108070, and 108082. If $P > 0.05$ or $(S = 0)$, then the null hypothesis is true, whereas if $P < 0.05$ or $(S = 1)$, then the alternative hypothesis is true. Inspecting those tables appears that our proposed algorithm could be

Table 15 Results of the Wilcoxon rank-sum test between IWOA and each algorithm on images from 61060:105053 under fitness values

Test image	h	SCA		WOA		SSA		FPA		FFA		L-SHADE		IMPA		EO		CSA	
		P	S	*P*	S	*P*	S	*P*	S	*P*	S	*P*	S	*P*	S	*P*	S	*P*	S
61060	2	<0.05	1	>0.05	0	>0.05	0	>0.05	0	>0.05	0	<0.05	1	>0.05	0	>0.05	0	<0.05	1
	3	>0.05	0	>0.05	0	>0.05	0	>0.05	0	>0.05	0	<0.05	1	>0.05	0	<0.05	1	<0.05	1
	4	<0.05	1	<0.05	1	<0.05	1	<0.05	1	<0.05	1	<0.05	1	>0.05	0	>0.05	0	<0.05	1
	5	<0.05	1	<0.05	1	<0.05	1	<0.05	1	<0.05	1	<0.05	1	>0.05	0	>0.05	0	<0.05	1
	10	<0.05	1	<0.05	1	<0.05	1	<0.05	1	<0.05	1	<0.05	1	>0.05	0	<0.05	1	<0.05	1
	20	<0.05	1	<0.05	1	<0.05	1	<0.05	1	<0.05	1	<0.05	1	<0.05	1	<0.05	1	<0.05	1
	40	<0.05	1	<0.05	1	<0.05	1	<0.05	1	<0.05	1	<0.05	1	<0.05	1	<0.05	1	<0.05	1
	60	<0.05	1	<0.05	1	<0.05	1	<0.05	1	<0.05	1	<0.05	1	<0.05	1	<0.05	1	<0.05	1
	80	<0.05	1	<0.05	1	<0.05	1	<0.05	1	<0.05	1	<0.05	1	<0.05	1	<0.05	1	<0.05	1
	100	<0.05	1	<0.05	1	<0.05	1	<0.05	1	<0.05	1	<0.05	1	<0.05	1	<0.05	1	<0.05	1
105053	2	<0.05	1	>0.05	0	>0.05	0	<0.05	1	>0.05	0	<0.05	1	>0.05	0	<0.05	1	<0.05	1
	3	<0.05	1	>0.05	0	<0.05	1	<0.05	1	>0.05	0	<0.05	1	>0.05	0	>0.05	0	<0.05	1
	4	<0.05	1	<0.05	1	>0.05	0	<0.05	1	>0.05	0	<0.05	1	>0.05	0	<0.05	1	<0.05	1
	5	<0.05	1	<0.05	1	<0.05	1	<0.05	1	<0.05	1	<0.05	1	<0.05	1	<0.05	1	<0.05	1
	10	<0.05	1	<0.05	1	<0.05	1	<0.05	1	<0.05	1	<0.05	1	<0.05	1	<0.05	1	<0.05	1
	20	<0.05	1	<0.05	1	<0.05	1	<0.05	1	<0.05	1	<0.05	1	<0.05	1	<0.05	1	<0.05	1
	40	<0.05	1	<0.05	1	<0.05	1	<0.05	1	<0.05	1	<0.05	1	<0.05	1	<0.05	1	<0.05	1
	60	<0.05	1	<0.05	1	<0.05	1	<0.05	1	<0.05	1	<0.05	1	<0.05	1	<0.05	1	<0.05	1
	80	<0.05	1	<0.05	1	<0.05	1	<0.05	1	<0.05	1	<0.05	1	<0.05	1	<0.05	1	<0.05	1
	100	<0.05	1	<0.05	1	<0.05	1	<0.05	1	<0.05	1	<0.05	1	<0.05	1	<0.05	1	<0.05	1

Table 16 Results of the Wilcoxon rank-sum test between IWOA and each algorithm on images from 181079:157055 under fitness values

Test image	h	SCA		WOA		SSA		FPA		FFA		L-SHADE		IMPA		EO		CSA	
		P	**S**	**P**	**S**	**P**	**S**	**P**	**S**	**P**	**S**	**P**	**S**	**P**	**S**	**P**	**S**	**P**	**S**
181079	2	<0.05	1	<0.05	1	<0.05	1	>0.05	0	>0.05	0	<0.05	1	>0.05	0	>0.05	0	>0.05	0
	3	<0.05	1	<0.05	1	<0.05	1	<0.05	1	>0.05	0	<0.05	1	>0.05	0	<0.05	1	<0.05	1
	4	<0.05	1	<0.05	1	<0.05	1	<0.05	1	<0.05	1	<0.05	1	<0.05	1	<0.05	1	<0.05	1
	5	<0.05	1	<0.05	1	<0.05	1	<0.05	1	<0.05	1	<0.05	1	<0.05	1	<0.05	1	<0.05	1
	10	<0.05	1	<0.05	1	<0.05	1	<0.05	1	<0.05	1	<0.05	1	<0.05	1	<0.05	1	<0.05	1
	20	<0.05	1	<0.05	1	<0.05	1	<0.05	1	<0.05	1	<0.05	1	<0.05	1	<0.05	1	<0.05	1
	40	<0.05	1	<0.05	1	<0.05	1	<0.05	1	<0.05	1	<0.05	1	<0.05	1	<0.05	1	<0.05	1
	60	<0.05	1	<0.05	1	<0.05	1	<0.05	1	<0.05	1	<0.05	1	<0.05	1	<0.05	1	<0.05	1
	80	<0.05	1	<0.05	1	<0.05	1	<0.05	1	<0.05	1	<0.05	1	<0.05	1	<0.05	1	<0.05	1
	100	<0.05	1	<0.05	1	<0.05	1	<0.05	1	<0.05	1	<0.05	1	<0.05	1	<0.05	1	<0.05	1
232038	2	<0.05	1	<0.05	1	>0.05	0	<0.05	1	>0.05	0	<0.05	1	>0.05	0	>0.05	0	>0.05	0
	3	<0.05	1	<0.05	1	<0.05	1	<0.05	1	>0.05	0	<0.05	1	>0.05	0	>0.05	0	<0.05	1
	4	<0.05	1	<0.05	1	<0.05	1	<0.05	1	<0.05	1	<0.05	1	>0.05	0	<0.05	1	<0.05	1
	5	<0.05	1	<0.05	1	<0.05	1	<0.05	1	<0.05	1	<0.05	1	>0.05	0	<0.05	1	<0.05	1
	10	<0.05	1	<0.05	1	<0.05	1	<0.05	1	<0.05	1	<0.05	1	>0.05	0	<0.05	1	<0.05	1
	20	<0.05	1	<0.05	1	<0.05	1	<0.05	1	<0.05	1	<0.05	1	<0.05	1	<0.05	1	<0.05	1
	40	<0.05	1	<0.05	1	<0.05	1	<0.05	1	<0.05	1	<0.05	1	<0.05	1	<0.05	1	<0.05	1
	60	<0.05	1	<0.05	1	<0.05	1	<0.05	1	<0.05	1	<0.05	1	<0.05	1	<0.05	1	<0.05	1
	80	<0.05	1	<0.05	1	<0.05	1	<0.05	1	<0.05	1	<0.05	1	<0.05	1	<0.05	1	<0.05	1
	100	<0.05	1	<0.05	1	<0.05	1	<0.05	1	<0.05	1	<0.05	1	<0.05	1	<0.05	1	<0.05	1

Table 16 (continued)

Test image	h	SCA		WOA		SSA		FPA		FFA		L-SHADE		IMPA		EO		CSA	
		P	**S**	**P**	**S**	**P**	**S**	**P**	**S**	**P**	**S**	**P**	**S**	**P**	**S**	**P**	**S**	**P**	**S**
277095	2	<0.05	1	<0.05	1	>0.05	0	<0.05	1	>0.05	0	<0.05	1	>0.05	0	>0.05	0	<0.05	1
	3	<0.05	1	<0.05	1	<0.05	1	<0.05	1	>0.05	0	<0.05	1	<0.05	1	>0.05	0	<0.05	1
	4	<0.05	1	<0.05	1	<0.05	1	<0.05	1	<0.05	1	<0.05	1	>0.05	0	>0.05	0	<0.05	1
	5	<0.05	1	<0.05	1	<0.05	1	<0.05	1	<0.05	1	<0.05	1	>0.05	0	<0.05	1	<0.05	1
	10	<0.05	1	<0.05	1	<0.05	1	<0.05	1	<0.05	1	<0.05	1	<0.05	1	<0.05	1	<0.05	1
	20	<0.05	1	<0.05	1	<0.05	1	<0.05	1	<0.05	1	<0.05	1	<0.05	1	<0.05	1	<0.05	1
	40	<0.05	1	<0.05	1	<0.05	1	<0.05	1	<0.05	1	<0.05	1	<0.05	1	<0.05	1	<0.05	1
	60	<0.05	1	<0.05	1	<0.05	1	<0.05	1	<0.05	1	<0.05	1	<0.05	1	<0.05	1	<0.05	1
	80	<0.05	1	<0.05	1	<0.05	1	<0.05	1	<0.05	1	<0.05	1	<0.05	1	<0.05	1	<0.05	1
	100	<0.05	1	<0.05	1	<0.05	1	<0.05	1	<0.05	1	<0.05	1	<0.05	1	<0.05	1	<0.05	1
299091	2	<0.05	1	<0.05	1	>0.05	0	<0.05	1	>0.05	0	<0.05	1	>0.05	0	>0.05	0	>0.05	0
	3	<0.05	1	<0.05	1	<0.05	1	<0.05	1	>0.05	0	<0.05	1	>0.05	0	>0.05	0	<0.05	1
	4	<0.05	1	<0.05	1	<0.05	1	<0.05	1	<0.05	1	<0.05	1	>0.05	0	>0.05	0	<0.05	1
	5	<0.05	1	<0.05	1	<0.05	1	<0.05	1	<0.05	1	<0.05	1	<0.05	1	<0.05	1	<0.05	1
	10	<0.05	1	<0.05	1	<0.05	1	<0.05	1	<0.05	1	<0.05	1	<0.05	1	<0.05	1	<0.05	1
	20	<0.05	1	<0.05	1	<0.05	1	<0.05	1	<0.05	1	<0.05	1	<0.05	1	<0.05	1	<0.05	1
	40	<0.05	1	<0.05	1	<0.05	1	<0.05	1	<0.05	1	<0.05	1	<0.05	1	<0.05	1	<0.05	1
	60	<0.05	1	<0.05	1	<0.05	1	<0.05	1	<0.05	1	<0.05	1	<0.05	1	<0.05	1	<0.05	1
	80	<0.05	1	<0.05	1	<0.05	1	<0.05	1	<0.05	1	<0.05	1	<0.05	1	<0.05	1	<0.05	1
	100	<0.05	1	<0.05	1	<0.05	1	<0.05	1	<0.05	1	<0.05	1	<0.05	1	<0.05	1	<0.05	1

Table 16 (continued)

Test image	h	SCA		WOA		SSA		FPA		FFA		L-SHADE		IMPA		EO		CSA	
		P	**S**	**P**	**S**	**P**	**S**	**P**	**S**	**P**	**S**	**P**	**S**	**P**	**S**	**P**	**S**	**P**	**S**
157055	2	<0.05	1	<,0.05	1	>0.05	0	<0.05	1	>0.05	0	<0.05	1	>0.05	0	>0.05	0	<0.05	1
	3	<0.05	1	<0.05	1	>0.05	0	<0.05	1	>0.05	0	<0.05	1	>0.05	0	>0.05	0	>0.05	0
	4	<0.05	1	<0.05	1	<0.05	1	<0.05	1	<0.05	1	<0.05	1	>0.05	0	>0.05	0	<0.05	1
	5	<0.05	1	<0.05	1	<0.05	1	<0.05	1	<0.05	1	<0.05	1	<0.05	1	>0.05	0	<0.05	1
	10	<0.05	1	<0.05	1	<0.05	1	<0.05	1	<0.05	1	<0.05	1	<0.05	1	<0.05	1	<0.05	1
	20	<0.05	1	<0.05	1	<0.05	1	<0.05	1	<0.05	1	<0.05	1	<0.05	1	<0.05	1	<0.05	1
	40	<0.05	1	<0.05	1	<0.05	1	<0.05	1	<0.05	1	<0.05	1	<0.05	1	<0.05	1	<0.05	1
	60	<0.05	1	<0.05	1	<0.05	1	<0.05	1	<0.05	1	<0.05	1	<0.05	1	<0.05	1	<0.05	1
	80	<0.05	1	<0.05	1	<0.05	1	<0.05	1	<0.05	1	<0.05	1	<0.05	1	<0.05	1	<0.05	1
	100	<0.05	1	<0.05	1	<0.05	1	<0.05	1	<0.05	1	<0.05	1	<0.05	1	<0.05	1	<0.05	1

Table 17 Results of the Wilcoxon rank-sum test between IWOA and each algorithm on images from 108070:med3 under fitness values

Test image	h	SCA		WOA		SSA		FPA		FFA		L-SHADE		IMPA		EO		CSA	
		P	**S**	**P**	**S**	**P**	**S**	**P**	**S**	**P**	**S**	**P**	**S**	**P**	**S**	**P**	**S**	**P**	**S**
108070	2	<0.05	1	>0.05	0	<0.05	1	>0.05	0	>0.05	0	<0.05	1	>0.05	0	>0.05	0	>0.05	0
	3	<0.05	1	<0.05	1	<0.05	1	<0.05	1	<0.05	1	<0.05	1	>0.05	0	>0.05	0	>0.05	0
	4	<0.05	1	<0.05	1	<0.05	1	<0.05	1	<0.05	1	<0.05	1	>0.05	0	<0.05	1	<0.05	1
	5	<0.05	1	<0.05	1	<0.05	1	<0.05	1	<0.05	1	<0.05	1	<0.05	1	<0.05	1	<0.05	1
	10	<0.05	1	<0.05	1	<0.05	1	<0.05	1	<0.05	1	<0.05	1	<0.05	1	<0.05	1	<0.05	1
	20	<0.05	1	<0.05	1	<0.05	1	<0.05	1	<0.05	1	<0.05	1	<0.05	1	<0.05	1	<0.05	1
	40	<0.05	1	<0.05	1	<0.05	1	<0.05	1	<0.05	1	<0.05	1	<0.05	1	<0.05	1	<0.05	1
	60	<0.05	1	<0.05	1	<0.05	1	<0.05	1	<0.05	1	<0.05	1	<0.05	1	<0.05	1	<0.05	1
	80	<0.05	1	<0.05	1	<0.05	1	<0.05	1	<0.05	1	<0.05	1	<0.05	1	<0.05	1	<0.05	1
	100	<0.05	1	<0.05	1	<0.05	1	<0.05	1	<0.05	1	<0.05	1	<0.05	1	<0.05	1	<0.05	1
108082	2	>0.05	0	>0.05	0	>0.05	0	>0.05	0	>0.05	0	<0.05	1	>0.05	0	>0.05	0	>0.05	0
	3	<0.05	1	<0.05	1	<0.05	1	<0.05	1	>0.05	0	<0.05	1	>0.05	0	>0.05	0	<0.05	1
	4	<0.05	1	<0.05	1	<0.05	1	<0.05	1	<0.05	1	<0.05	1	>0.05	0	>0.05	0	<0.05	1
	5	<0.05	1	<0.05	1	<0.05	1	<0.05	1	<0.05	1	<0.05	1	>0.05	0	<0.05	1	<0.05	1
	10	<0.05	1	<0.05	1	<0.05	1	<0.05	1	<0.05	1	<0.05	1	<0.05	1	<0.05	1	<0.05	1
	20	<0.05	1	<0.05	1	<0.05	1	<0.05	1	<0.05	1	<0.05	1	<0.05	1	<0.05	1	<0.05	1
	40	<0.05	1	<0.05	1	<0.05	1	<0.05	1	<0.05	1	<0.05	1	<0.05	1	<0.05	1	<0.05	1
	60	<0.05	1	<0.05	1	<0.05	1	<0.05	1	<0.05	1	<0.05	1	<0.05	1	<0.05	1	<0.05	1
	80	<0.05	1	<0.05	1	<0.05	1	<0.05	1	<0.05	1	<0.05	1	<0.05	1	<0.05	1	<0.05	1
	100	<0.05	1	<0.05	1	<0.05	1	<0.05	1	<0.05	1	<0.05	1	<0.05	1	<0.05	1	<0.05	1

significantly different from the others for most test images under threshold levels greater than 5 however, for threshold levels smaller than that, it could almost reach the same outcomes of some compared algorithms. Based on that, our proposed algorithm can outperform all other algorithms for most of the threshold levels with all the test images.

7 Conclusion and future directions

Image segmentation is considered a significant problem that attracts many researchers those days. Due to using image segmentation in solving many problems in the real world, researchers have been tried to find a better technique that enables them to extract the required information from the image. Many techniques were proposed, such as threshold-based, region-based, feature-based clustering, and, edge-based to resolve this research challenge. The threshold-based segmentation is used for analyzing the image segmentation due to its ease in use. To tackle the image segmentation problem using the threshold technique, we proposed an improvement on the standard whale optimization algorithm by proposing two strategies, namely linearly convergence increasing and local minima avoidance strategy (LCMA), and ranking-based updating method (RUM) that help the whale optimization algorithm (WOA) in accelerating the convergence toward the best-so-far solution and avoiding local minima that fall into at the end of the optimization process. LCMA moves the worst K particle towards the best so-far solution for accelerating the convergence and avoiding falling into local minima by updating them within the search space based on a certain probability. K starts with a small value at the start of the optimization and increases gradually with the increasing number of the iteration even reaching the maximum at the end of the iteration. Meanwhile, RUM utilizes each individual in the population as possible in an effective way that will gradually explore the solutions around the best-so-far solution as an attempt to reach better outcomes. The experiments are performed to observe the performance of IWOA with thresholds level between 2 and 100: the first one is based on a set of the normal images taken from Berkeley Segmentation Dataset (BSD). To see the superiority of IWOA, through these two experiments, it was compared with other existing algorithms like the standard whale optimization algorithm (WOA), sine-cosine algorithm (SCA), slap swarm algorithm (SSA), flower pollination algorithm (FPA), and L-SHADE algorithm, Firefly algorithm (FFA), Equilibrium optimizer (EO), and Crow search algorithm (CSA). The quality of segmented images, fitness values, and STD metrics obtained from each algorithm through these two experiments demonstrate that the proposed algorithm outperforms all algorithms integrated with the comparison. Despite these promising results, our algorithm could not outperform some algorithms in CPU time, as our main limitation. Therefore, our future extensin will be applying the LCMA technique with other evolutionary algorithms for reducing the running time and improving the quality of results. In addition, a version of the IWOA for solving the multi-objective and single-objective optimization problems is included in our future work. Moreover, a binary version of IWOA for overcoming the feature selection problem will be given as a work in the future.

Funding This research has no funding source.

Declarations

Conflict of interest The authors declare that there is no conflict of interest about the research.

Ethical approval This article does not contain any studies with human participants or animals performed by any of the authors.

References

Abd El Aziz M, Ewees AA, Hassanien AE (2017) Whale optimization algorithm and moth-flame optimization for multilevel thresholding image segmentation. Expert Syst Appl 83:242–256

Abd El Aziz M, Ewees AA, Hassanien AE, Mudhsh M, Xiong S (2018) Multi-objective whale optimization algorithm for multilevel thresholding segmentation. In: Advances in soft computing and machine learning in image processing. Springer, Cham, pp. 23–39

Abdel-Basset M, Manogaran G, El-Shahat D, Mirjalili S (2018) Integrating the whale algorithm with tabu search for quadratic assignment problem: a new approach for locating hospital departments. Appl Soft Comput 73:530–546

Abdel-Basset M, Chang V, Mohamed R (2020) Hsma_woa: a hybrid novel slime mould algorithm with whale optimization algorithm for tackling the image segmentation problem of chest x-ray images. Appl Soft Comput 95:106642

Abdel-Basset M, Mohamed R, Mirjalili S, Chakrabortty RK, Ryan MJ (2020) Solar photovoltaic parameter estimation using an improved equilibrium optimizer. Sol Energy 209:694–708

Abdel-Basset M, Mohamed R, Sallam KM, Chakrabortty RK, Ryan MJ (2020) An efficient-assembler whale optimization algorithm for DNA fragment assembly problem: analysis and validations. IEEE Access 8:222 144–222 167

Abdel-Basset M, Mohamed R, Elhoseny M, Chakrabortty RK, Ryan M (2020) A hybrid covid-19 detection model using an improved marine predators algorithm and a ranking-based diversity reduction strategy. IEEE Access 8:79 521–79 540

Abdel-Basset M, Chang V, Mohamed R (2021) A novel equilibrium optimization algorithm for multi-thresholding image segmentation problems. Neural Comput Appl 33(17):10 685–10 718

Abdel-Basset M, Mohamed R, Abouhawwash M (2021) Balanced multi-objective optimization algorithm using improvement based reference points approach. Swarm Evol Comput 60:100791

Abdel-Basset M, Mohamed R, Mirjalili S (2020) A binary equilibrium optimization algorithm for 0–1 knapsack problems. Comput Ind Eng 151:106946

Aksac A, Ozyer T, Alhajj R (2017) Complex networks driven salient region detection based on superpixel segmentation. Pattern Recogn 66:268–279

Alberti M, Seuret M, Pondenkandath V, Ingold R, Liwicki M (2017) "Historical document image segmentation with lda-initialized deep neural networks," In: Proceedings of the 4th international workshop on historical document imaging and processing, pp 95–100

Al-Musawi AK, Anayi F, Packianather M (2020) Three-phase induction motor fault detection based on thermal image segmentation. Infra Phys Technol 104:103140

Bal A, Banerjee M, Sharma P, Maitra M (2020) Gray matter segmentation and delineation from positron emission tomography (pet) image. In: Emerging technology in modelling and graphics. Springer, Singapore, pp 359–372

Bao X, Jia H, Lang C (2019) A novel hybrid harris hawks optimization for color image multilevel thresholding segmentation. Ieee Access 7:76 529-76 546

Barman R, Ehrmann M, Clematide S, Oliveira SA, Kaplan F (2020) "Combining visual and textual features for semantic segmentation of historical newspapers," *arXiv preprint*arXiv:2002.06144

Bhandari AK, Kumar IV (2019) A context sensitive energy thresholding based 3D OTSU function for image segmentation using human learning optimization. Appl Soft Comput 82:105570

Bhandari AK, Singh VK, Kumar A, Singh GK (2014) Cuckoo search algorithm and wind driven optimization based study of satellite image segmentation for multilevel thresholding using kapur's entropy. Expert Syst Appl 41(7):3538–3560

Brest J, Maučec MS, Bošković B (2016) "il-shade: improved l-shade algorithm for single objective real-parameter optimization," In: 2016 IEEE congress on evolutionary computation (CEC). IEEE, pp 1188–1195

Chakraborty F, Nandi D, Roy PK (2019) Oppositional symbiotic organisms search optimization for multilevel thresholding of color image. Appl Soft Comput 82:105577
Chen G (2020) Image segmentation algorithm combined with regularized pm de-noising model and improved watershed algorithm. J Med Imag Health Informat 10(2):515–521
Chouksey M, Jha RK, Sharma R (2020) A fast technique for image segmentation based on two meta-heuristic algorithms. Multimed Tools Appl 79(27):19075–19127
Cuevas E, Fausto F, González A (2020) Locust search algorithm applied to multi-threshold segmentation. In: New advancements in swarm algorithms: operators and applications. Springer, Cham, pp 211–240
De S, Dey S, Debnath S, Deb A (2020) "A new modified red deer algorithm for multi-level image thresholding," In: 2020 Fifth international conference on research in computational intelligence and communication networks (ICRCICN). IEEE, pp 105–111
Di Martino F, Sessa S (2020) Pso image thresholding on images compressed via fuzzy transforms. Inf Sci 506:308–324
Dirami A, Hammouche K, Diaf M, Siarry P (2013) Fast multilevel thresholding for image segmentation through a multiphase level set method. Signal Process 93(1):139–153
Egiazarian K, Astola J, Ponomarenko N, Lukin V, Battisti F, Carli M (2006) "New full-reference quality metrics based on hvs," In: Proceedings of the second international workshop on video processing and quality metrics, vol. 4
El-Fergany AA, Hasanien HM, Agwa AM (2019) Semi-empirical PEM fuel cells model using whale optimization algorithm. Energy Convers Manage 201:112197
Elsayed SM, Sarker RA, Essam DL (2014) A new genetic algorithm for solving optimization problems. Eng Appl Artif Intell 27:57–69
Erdmann H, Wachs-Lopes G, Gallão C, Ribeiro MP, Rodrigues PS (2015) A study of a firefly meta-heuristics for multithreshold image segmentation. In: Developments in medical image processing and computational vision. Springer, Cham, pp 279–295
Farook TH, Mousa MA, Jamayet NB (2020) Method to control tongue position and open source image segmentation for cone-beam computed tomography of patients with large palatal defect to facilitate digital obturator design. J Oral Maxillofac Surg Med Pathol 32(1):61–64
Ghamisi P, Couceiro MS, Martins FM, Benediktsson JA (2013) Multilevel image segmentation based on fractional-order darwinian particle swarm optimization. IEEE Trans Geosci Remote Sens 52(5):2382–2394
Griswold M, Jiang Y, Ma D, Deshmane A, Badve C, Gulani V, Sunshine JL (2019) U.S. Patent No. 10,261,154. U.S. Patent and Trademark Office, Washington, DC
Guo C, Li H (2007) "Multilevel thresholding method for image segmentation based on an adaptive particle swarm optimization algorithm," In: Australasian joint conference on artificial intelligence. Springer, pp 654–658
Han J, Yang C, Zhou X, Gui W (2017) A new multi-threshold image segmentation approach using state transition algorithm. Appl Math Model 44:588–601
Haynes W (2013) Wilcoxon rank sum test. Encyclopedia of systems biology, 2354–2355
He L, Huang S (2020) An efficient krill herd algorithm for color image multilevel thresholding segmentation problem. Appl Soft Comput 89:106063
Hore A, Ziou D (2010) "Image quality metrics: Psnr versus ssim," In: 2010 20th international conference on pattern recognition. IEEE, pp 2366–2369
Huo F, Sun X, Ren W (2020) Multilevel image threshold segmentation using an improved bloch quantum artificial bee colony algorithm. Multimed Tools Appl 79(3):2447–2471
Hu R, Rohrbach M, Venugopalan S, Darrell T (2016) "Utilizing large scale vision and text datasets for image segmentation from referring expressions," *arXiv preprint*arXiv:1608.08305
Jafari-Asl J, Seghier MEAB, Ohadi S, van Gelder P (2021) Efficient method using whale optimization algorithm for reliability-based design optimization of labyrinth spillway. Appl Soft Comput 101:107036
Kandhway P, Bhandari AK (2019) Spatial context cross entropy function based multilevel image segmentation using multi-verse optimizer. Multimed Tools Appl 78(16):22 613–22 641
Kapur JN, Sahoo PK, Wong AK (1985) A new method for gray-level picture thresholding using the entropy of the histogram. Computer Vis Gr Image Process 29(3):273–285
Karydas CG (2020) Optimization of multi-scale segmentation of satellite imagery using fractal geometry. Int J Remote Sens 41(8):2905–2933
Kaveh A, Talatahari S (2010) An improved ant colony optimization for constrained engineering design problems. Engineering Computations
Khairuzzaman AKM, Chaudhury S (2017) Multilevel thresholding using grey wolf optimizer for image segmentation. Expert Syst Appl 86:64–76

Kuruvilla J, Sukumaran D, Sankar A, Joy SP (2016) "A review on image processing and image segmentation," In: 2016 international conference on data mining and advanced computing (SAPIENCE). IEEE, pp 198–203

Lang C, Jia H (2019) Kapur's entropy for color image segmentation based on a hybrid whale optimization algorithm. Entropy 21(3):318

Li K, Tan Z (2019) An improved flower pollination optimizer algorithm for multilevel image thresholding. IEEE Access 7:165 571–165 582

Liu Y, Mu C, Kou W, Liu J (2015) Modified particle swarm optimization-based multilevel thresholding for image segmentation. Soft Comput 19(5):1311–1327

Liu M, Yao X, Li Y (2020) Hybrid whale optimization algorithm enhanced with lévy flight and differential evolution for job shop scheduling problems. Appl Soft Comput 87:105954

Liu Y, Hu K, Zhu Y, Chen H (2015) "Color image segmentation using multilevel thresholding-cooperative bacterial foraging algorithm," In: 2015 IEEE International conference on cyber technology in automation, control, and intelligent systems (CYBER). IEEE, pp 181–185

Mafarja M, Mirjalili S (2018) Whale optimization approaches for wrapper feature selection. Appl Soft Comput 62:441–453

Maitra M, Chatterjee A (2008) A hybrid cooperative-comprehensive learning based pso algorithm for image segmentation using multilevel thresholding. Expert Syst Appl 34(2):1341–1350

Manikandan S, Ramar K, Iruthayarajan MW, Srinivasagan K (2014) Multilevel thresholding for segmentation of medical brain images using real coded genetic algorithm. Measurement 47:558–568

Mirjalili S (2016) Sca: a sine cosine algorithm for solving optimization problems. Knowl-Based Syst 96:120–133

Mirjalili S, Lewis A (2016) The whale optimization algorithm. Adv Eng Softw 95:51–67

Mittal M, Arora M, Pandey T, Goyal LM (2020) "Image segmentation using deep learning techniques in medical images," In: Advancement of machine intelligence in interactive medical image analysis. Springer, pp 41–63

Moses MML (2020) "Coyote optimization algorithm based multilevel thresholding approach for image segmentation," J Soft Comput Eng Appl 1(2)

Mostafa A, Hassanien AE, Houseni M, Hefny H (2017) Liver segmentation in mri images based on whale optimization algorithm. Multimed Tools Appl 76(23):24 931–24 954

Naji Alwerfali HS, Al-qaness MA, Abd Elaziz M, Ewees AA, Oliva D, Lu S (2020) Multi-level image thresholding based on modified spherical search optimizer and fuzzy entropy. Entropy 22(3):328

Naoum A, Nothman J, Curran J (2019) "Article segmentation in digitised newspapers with a 2d markov model," In: 2019 International conference on document analysis and recognition (ICDAR). IEEE, pp 1007–1014

Narayanan BN, Hardie RC, Kebede TM, Sprague MJ (2019) Optimized feature selection-based clustering approach for computer-aided detection of lung nodules in different modalities. Pattern Anal Appl 22(2):559–571

Oliva D, Hinojosa S, Cuevas E, Pajares G, Avalos O, Gálvez J (2017) Cross entropy based thresholding for magnetic resonance brain images using crow search algorithm. Expert Syst Appl 79:164–180

Oliva D, Abd Elaziz M, Hinojosa S (2019) Fuzzy entropy approaches for image segmentation. In: Metaheuristic algorithms for image segmentation: theory and applications. Springer, Cham, pp 141–147

Otsu N (1979) A threshold selection method from gray-level histograms. IEEE Trans Syst Man Cybern 9(1):62–66

Pan Y, Xia Y, Zhou T, Fulham M (2017) Cell image segmentation using bacterial foraging optimization. Appl Soft Comput 58:770–782

Prathusha P, Jyothi S (2018) A novel edge detection algorithm for fast and efficient image segmentation. In: Data engineering and intelligent computing. Springer, Singapore, pp 283–291

Ren T, Wang H, Feng H, Xu C, Liu G, Ding P (2019) Study on the improved fuzzy clustering algorithm and its application in brain image segmentation. Appl Soft Comput 81:105503

Sanyal N, Chatterjee A, Munshi S (2011) An adaptive bacterial foraging algorithm for fuzzy entropy based image segmentation. Expert Syst Appl 38(12):15 489–15 498

Saremi S, Mirjalili SZ, Mirjalili SM (2015) Evolutionary population dynamics and grey wolf optimizer. Neural Comput Appl 26(5):1257–1263

Sathya P, Kayalvizhi R (2011) Modified bacterial foraging algorithm based multilevel thresholding for image segmentation. Eng Appl Artif Intell 24(4):595–615

Shahabi F, Pourahangarian F, Beheshti H (2019) A multilevel image thresholding approach based on crow search algorithm and Otsu method. J Dec Op Res 4(1):33–41

Sikariwal P, Chanak P (2018) “An efficient moth flame optimization algorithm based multi level thresholding for segmentation of satellite images,” In: 2018 Second international conference on intelligent computing and control systems (ICICCS). IEEE, pp 269–274
Singla A, Patra S (2017) A fast automatic optimal threshold selection technique for image segmentation. SIViP 11(2):243–250
Sinha P, Tuteja M, Saxena S (2020) Medical image segmentation: hard and soft computing approaches. SN Appl Sci 2(2):1–8
Song Y, Liu P (2020) Segmentation of sonar images with intensity inhomogeneity based on improved mrf. Appl Acoust 158:107051
Su T, Zhang S (2017) Local and global evaluation for remote sensing image segmentation. ISPRS J Photogramm Remote Sens 130:256–276
Tang K, Xiao X, Wu J, Yang J, Luo L (2017) An improved multilevel thresholding approach based modified bacterial foraging optimization. Appl Intell 46(1):214–226
Upadhyay P, Chhabra JK (2020) Kapur’s entropy based optimal multilevel image segmentation using crow search algorithm. Applied soft computing 97:105522
Wang R, Zhou Y, Zhao C, Wu H (2015) A hybrid flower pollination algorithm based modified randomized location for multi-threshold medical image segmentation. Bio-Med Mater Eng 26(s1):S1345–S1351
Wang S, Jia H, Peng X (2020) Modified salp swarm algorithm based multilevel thresholding for color image segmentation. Math Biosci Eng 17:700–724
Wang E, Tu D, Chen Y, Zhang F (2019) “An improved bacterial foraging strategy for image segmentation,” In: 2019 International conference on intelligent transportation, big data & smart city (ICITBS). IEEE, pp 544–547
Wang X, Wang X, Wilkes DM (2019) Machine learning-based natural scene recognition for mobile robot localization in an unknown environment. Springer
Xiang W (2011) Analysis of the time complexity of quick sort algorithm, In: 2011 international conference on information management, innovation management and industrial engineering, vol 1, pp 408–410
Xiong L, Tang G, Chen YC, Hu YX, Chen RS (2020) Color disease spot image segmentation algorithm based on chaotic particle swarm optimization and FCM. J Supercomput 76(11), 8756–8770
Yang X-S (2012) “Flower pollination algorithm for global optimization,” In: International conference on unconventional computing and natural computation. Springer, pp 240–249
Yan Z, Zhang J, Tang J (2020) Modified water wave optimization algorithm for underwater multilevel thresholding image segmentation. Multimed Tools Appl 79(43):32415–32448
Yao X, Li Z, Liu L, Cheng X (2019) “Multi-threshold image segmentation based on improved grey wolf optimization algorithm,” In: IOP Conference series: earth and environmental science, vol. 252, no. 4. IOP Publishing, p 042105
Yue X, Zhang H (2020) Modified hybrid bat algorithm with genetic crossover operation and smart inertia weight for multilevel image segmentation. Appl Soft Comput 90:106157
Zhang Y, Miao S, Mansi T, Liao R (2020) Unsupervised x-ray image segmentation with task driven generative adversarial networks. Med Image Anal 62:101664
Zhang Z, Wu C, Coleman S, Kerr D (2020) Dense-inception u-net for medical image segmentation. Comput Methods Programs Biomed 192:105395
Zhang H, Essa E, Xie X (2020) Automatic vessel lumen segmentation in optical coherence tomography (oct) images. Appl Soft Comput 88:106042

Authors and Affiliations

Mohamed Abdel-Basset[1] · Reda Mohamed[1] · Mohamed Abouhawwash[2,3]

Mohamed Abdel-Basset
mohamedbasset@ieee.org

Reda Mohamed
redamoh@zu.edu.eg

[1] Zagazig Univesitry, Shaibet an Nakareyah, Zagazig 2, Zagazig 44519, Ash Sharqia Governorate,

Egypt

[2] Department of Mathematics Faculty of Science, Mansoura University, Mansoura 35516, Egypt

[3] Department of Computational Mathematics, Science, and Engineering (CMSE), Michigan State University, East Lansing, MI 48824, USA